

# **CELLULOSE BASED THERMOCHROMIC SMART WINDOW SYSTEM**

by

**Sai Aranke**

**A Thesis**

*Submitted to the Faculty of Purdue University*

*In Partial Fulfillment of the Requirements for the degree of*

**Master of Science in Mechanical Engineering**



School of Mechanical Engineering

West Lafayette, Indiana

August 2021

**THE PURDUE UNIVERSITY GRADUATE SCHOOL**  
**STATEMENT OF COMMITTEE APPROVAL**

**Dr. Tian Li, Chair**

School of Mechanical Engineering

**Dr. Xuilin Ruan**

School of Mechanical Engineering

**Dr. Jeffery Youngblood**

School of Materials Engineering

**Dr. Athanasios Tzempelikos**

Lyles School of Civil Engineering

**Approved by:**

Dr. Nicole Key

*Dedicated to my loved ones.*

## **ACKNOWLEDGMENTS**

I wish to express my sincere gratitude to my advisor Prof. Tian Li for giving me the opportunity to be a member of her research team and for her patience, encouragement, and immense knowledge. I thank her for igniting the interest on a topic that was unfamiliar to me when I started my program. Her guidance helped me in all time of research and writing of this thesis.

Besides my advisor, I would like to thank the rest of my thesis committee, Prof. Jeffery Youngblood and Prof. Xiulin Ruan and Prof. Thanos Tzempelikos for their guidance, encouragement and insightful comments.

I acknowledge my colleague, friend and mentor, Dr. Chi Zhang. I would like to thank him for his generous guidance, motivation, and encouragement at every step of this thesis.

Family, friends and colleagues have been of a great support during the preparation of this thesis. I would like to thank my fellow lab mates Wenkai Zhu, Yun Zhang, Wenhui Xu, Xuan Li, Yanbing Wang, Heijia Zhang for stimulating discussions and help during some of my experiments.

## TABLE OF CONTENTS

LIST OF TABLES .....	7
LIST OF FIGURES .....	8
ABBREVIATIONS .....	9
ABSTRACT.....	10
1. INTRODUCTION .....	11
1.1 Background.....	11
1.2 Smart Window technologies .....	14
1.3 Outline of Thesis.....	18
1.4 Literature Review.....	19
1.4.1 Smart window technologies.....	19
1.4.2 Thermochromic windows .....	21
1.4.3 Cellulose hydrogels .....	24
2. THERMOCHROMIC SMART WINDOWS .....	26
2.1 Cellulose .....	26
2.2 Methyl Cellulose structure.....	29
2.3 Methyl Cellulose applications.....	30
2.4 Methyl Cellulose Gelation Mechanism .....	31
2.5 Methyl Cellulose solution thermodynamics .....	32
2.6 Methyl Cellulose LCST tunability.....	33
2.6.1 Degree of Substitution .....	33
2.6.2 Methyl Cellulose concentration.....	34
2.6.3 Anions.....	35
3. EXPERIMENTAL METHODS .....	38
3.1 Materials .....	38
3.2 Sample Preparation .....	38
3.3 Sample Characterization .....	39
3.3.1 Transition temperature measurement .....	39
3.3.2 UV-VIS Spectroscopy .....	39

3.3.3	Freezing Resistance Test .....	40
3.3.4	Scanning Electron Microscopy in cryogenic mode (Cryo-SEM).....	40
3.3.5	Dynamic Light Scattering.....	41
3.3.6	Window demonstration.....	41
4.	RESULTS AND DISCUSSION.....	42
4.1	Transition temperature .....	42
4.2	UV-VIS Spectroscopy .....	43
4.3	Effect of Salts.....	47
4.4	Freeze Resistance.....	51
4.5	Size distribution .....	54
4.6	Scanning Electron Microscopy .....	58
4.7	Window demonstration.....	61
5.	CONCLUSION.....	63
5.1	Conclusions.....	63
5.2	Future Works .....	65
	REFERENCES .....	67

## LIST OF TABLES

Table 1 Energy flow in building shells (Quads) <sup>7</sup> .....	13
Table 2 Comparison of Thermo-, Electro-, and Photo- chromic windows <sup>28</sup> .....	21
Table 3 Integral Transmittance % for 15,25, 35g/L MC samples as a function of temperature... 47	
Table 4 Radii and free energies of hydration for selected ions <sup>80</sup> .....	50
Table 5 Freeze resistance of pure MC aqueous solutions of varying MC concentrations.....	52
Table 6 Freeze resistance of MC aqueous solutions with 0.4 M and 0.6 M NaF .....	53

## LIST OF FIGURES

Figure 1 U.S. total energy consumption by end-use sector in 1950 through 2020 <sup>4,5</sup> .....	12
Figure 2 End use energy consumption shares by U.S homes, 2015 <sup>5</sup> .....	12
Figure 3 Classification of smart window technologies.....	15
Figure 4 Typical configuration of thermochromic windows .....	16
Figure 5 Solar Spectrum on Earth.....	17
Figure 6 Advantages of cellulose.....	27
Figure 7 Structure of Cellulose .....	29
Figure 8 Structure of Methy Cellulose.....	30
Figure 9 Clear and Opaque states of a MC aqueous solution .....	32
Figure 10 Gelation mechanism of MC solution for low (top) and high (bottom) concentrations of MC. Part (a) shows state of MC chains at temperature below the LCST of cellulose. (b) shows temperatures higher than LCST. ....	35
Figure 11 Hofmeister series: ions on the left producing a salting in (stabilizing) effect on the polymer, whereas ions on right lead to salting out (stabilizing) effect.....	36
Figure 12 States of a 25g/L MC sample at increasing temperatures .....	42
Figure 13 Transition temperature of MC as a function of MC concentration .....	43
Figure 14 Transmittance of methyl cellulose at temperatures between 20oC – 70oC for a) 15g/L b) 25g/L c) 35 g/L methyl cellulose concentration .....	44
Figure 15 Transmittance of 15,25, 35g/L MC samples as a function of temperature .....	46
Figure 16 25g/L MC solution percipitation in presence of $Na_2CO_3$ , $Na_2SO_4$ , $Na_2S_2O_3$ .....	48
Figure 17 Change in transition temperature for a 25 g/L MC aqueous solution with the concentration of various sodium salts.....	49
Figure 18 Particle size distribution of 10 g/L MC sample at a) 20oC and b) 70oC using DLS	55
Figure 19 Particle size distribution of 15 gL MC sample at a) 20oC and b) 70oC using DLS .	56
Figure 20 Cryo-SEM micrographs of the porous network formed within the 25 g/L MC hydrogels. ....	58
Figure 21 Mechanism for the freezing process of the sample when using slushy nitrogen for sample preparation for cryo-SEM .....	60
Figure 22 Model thermochromic window demonstration a) without sunlight exposure b) after exposure to solar radiation .....	61



## **ABBREVIATIONS**

AGU	Anhydro glucose unit
ASHRAE	American Society of Heating Refrigeration and Air Conditioning
DLS	Dynamic Light Scattering
DOE	Department of Energy
EC	Electrochromic
HVAC	Heating Ventilation and Air Conditioning
LCST	Lower Critical Solution Temperature
MC	Methyl Cellulose
PC	Photochromic
SEM	Scanning Electron Microscopy

## ABSTRACT

Smart windows that modulate solar radiation by changing their optical state in response to temperature stimulus are developing as promising solutions towards reducing the energy consumption of buildings. The market adoption of such systems has been slow due to the barriers in scalability, cost, as well as complexity in their integration into existing systems. Aiming these features, we have proposed a retrofit smart window design based on the temperature-responsive polymer Methyl Cellulose (MC). The system utilizes a sustainable, earth abundant and cost-effective cellulose based thermo-responsive material to transform existing windows to a thermally dynamic smart window system. The observed optical change of MC from transparent to opaque state is dependent on temperature and is triggered by the thermodynamic mechanism of reversible coil-globule transition, which results in a stable performance of the proposed device. Its solar modulation ability was studied using ultraviolet-visible- spectroscopy. Effect of MC concentration and various salts on the optical performance were investigated. It was found that the transition temperature the polymer can be tuned by varying MC concentration and by adding salts to the system. The tunability of transition temperature is a function of the concentration of salt and the type of anion in the salt. It was observed that the transition temperature of the window can be tuned between  $35^{\circ}\text{C}$  to  $70^{\circ}\text{C}$  , allowing a wide range of control over switching temperature. Controllable LCST, low freezing point, sustainable base material, scalable production, low cost, retrofit system makes them ideal candidates for smart window applications.

# **1. INTRODUCTION**

## **1.1 Background**

In recent years, growing population and modernization have dramatically increased the energy demand.<sup>1</sup> Building sector is one of the largest consumers of energy. The EIA (Energy Information Administration) has designated all energy consumption activities in the U.S into four major sectors: transportation, industrial processes, commercial buildings and residential buildings. It is estimated that building energy consumption accounts to up to 40% of the overall energy usage, surpassing the energy requirements of industrial and transportation sectors.<sup>2,3</sup> Figure 1 shows the energy consumption trends of the four main sectors between years 1950 through 2020. It can be seen that the energy demands of the commercial and residential sector has increased drastically over years. Residential Energy Consumption survey (RECS) conducted by EIA in 2015 reported that, on average, more than half (51% in 2015) of the residential energy consumption is for space heating and air conditioning purposes. Building space conditioning systems such as the heating, ventilation and air conditioning (HVAC) consume between 42~68% of the total building energy depending on the depending on the geographic locations and environmental conditions.<sup>1</sup> It is estimated that the energy requirements of HVAC system will see a rise of 7% per year, on average, between years 2020 and 2030. Most of the building structures are used for decades. Thus, reducing their energy consumption will not only ensure energy cost saving but also will be a meaningful step towards climate change mitigation. Use of novel materials and system can help lower the cooling requirements of buildings and reduce the consumption of electricity and fossil fuels. Thus, energy efficient building technologies are gaining increasing scientific interest to decrease the building energy consumption while maintaining building comfort levels.

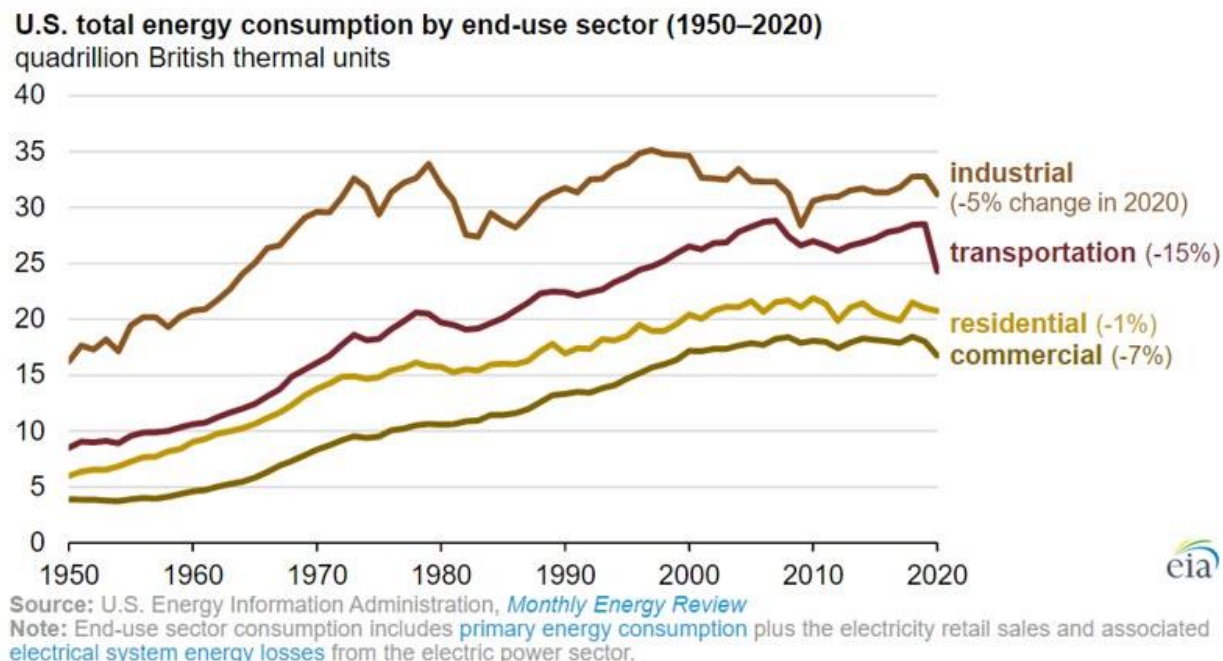


Figure 1 U.S. total energy consumption by end-use sector in 1950 through 2020 <sup>4,5</sup>

#### End use energy consumption shares by U.S homes, 2015

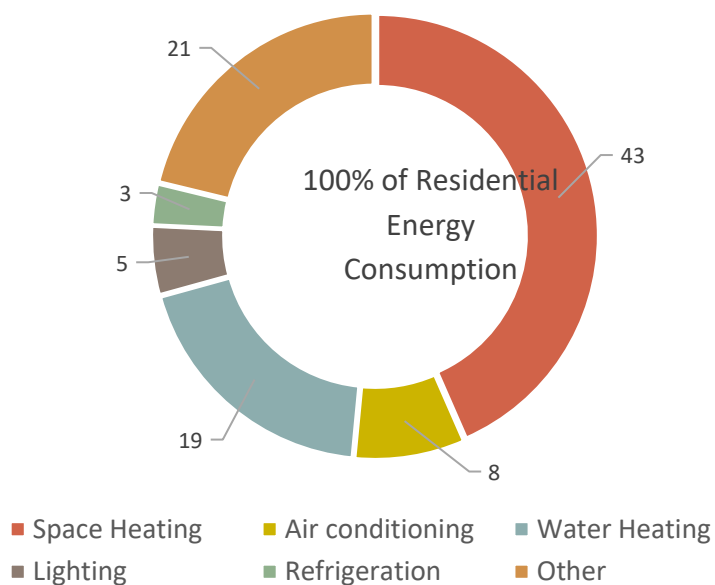


Figure 2 End use energy consumption shares by U.S homes, 2015<sup>5</sup>

Controlling the solar radiation entering the building spaces can help achieve indoor wellbeing and improve the overall energy efficiency of the building. Windows are important part of the building envelop. Windows allow sunlight to enter the building and ensure sufficient daylight for the occupant to keep them healthy and efficient.<sup>6</sup> Serving as the main channel of heat exchange, windows are the least efficient parts of a building.<sup>3</sup> The U.S. Department of Energy (DOE) has reported that 60% of the energy flow in the building occurs through the building envelope components, that include walls, windows, roof and the foundation.<sup>7</sup> Table 1 shows the average heat flow through different building envelope components in residential and commercial buildings. Virtually the entire commercial energy cooling load comes from the energy entering through the windows (i.e., solar heat gain). Although infiltration plays a significant role, a large portion of residential cooling results from the window heat gain.<sup>7</sup>

Table 1 Energy flow in building shells (Quads)<sup>7</sup>

Building component	Residential		Commercial	
	Heating	Cooling	Heating	Cooling
Roofs	1.00	0.49	0.88	0.05
Walls	1.54	0.34	1.48	-0.03
Foundation	1.17	-0.22	0.79	-0.21
Infiltration	2.26	0.03	1.29	-0.15
Windows (conduction)	2.06	0.03	1.6	-0.3
Windows (solar heat gain)	-0.66	1.44	-0.97	1.38

Many passive coating technologies exist, which when applied to the window can modify the energy efficiency by managing the heat gain or loss. However, dynamic and adaptive window technologies, such as smart windows, are gaining significant attention as they are effective and practical to use in locations with varying weather and offer potential for significant energy savings. ‘Smart Window’ refers to a system that can intelligently modulate the transmission of ultraviolet (UV), visible, Infrared (IR) solar radiations in response to stimuli like heat, light, voltage, and gas. Thus, based on the type of stimuli, smart windows are classified as thermochromic, photochromic, electrochromic and gas chromic. Previous simulations have projected that the use of smart can decrease the energy consumption of a building by up to 40% as compared to static windows.<sup>8</sup>

## **1.2 Smart Window technologies**

Smart windows are classified into two broad categories: passive and active. Passive subcategory includes photochromic and thermochromic windows. Active subcategory includes electrochromic, polymer dispersed liquid crystal and suspended particle device windows. Passive window technologies use natural or non-electric stimuli, such as heat and light to transition from dark to light visual state and vis versa. Thermochromic windows use the heat from the sunlight to tint the windows. Photochromic windows change transparency in response to the intensity of light. Active window technologies use electrical stimulus to change the visual state of the window. Electrochromic windows switch their color in response to an applied external DC voltage. Such windows consist of Lithium ions that migrate between two electrodes through a separator. When voltage is applied to such windows, the ions migrate from the separator to the outer electrode, where they scatter the incoming light and make the window appear opaque. The polymer dispersed liquid crystal window technologies employ liquid crystals that respond to an externally applied AC power. The suspended rod-shaped particles are placed between two glass substrates and are free to float between the glass substrates. When voltage is applied to the window, the rod-shaped particles align in a single direction allowing light to pass through the window. When the voltage applied is removed, the particle orients randomly, blocking the incident light from passing through the window. Suspended particle device window technology consists of suspended particles encapsulated in polymer. Such window responds to an AC current and switch from liquid to opaque states within milliseconds. When no voltage is applied to the window, the suspended particles remains randomly oriented and scatter the incident light giving it a milky white appearance. When voltage is applied to the system, the crystals align in the direction of the electric field and allow light to pass through the window.

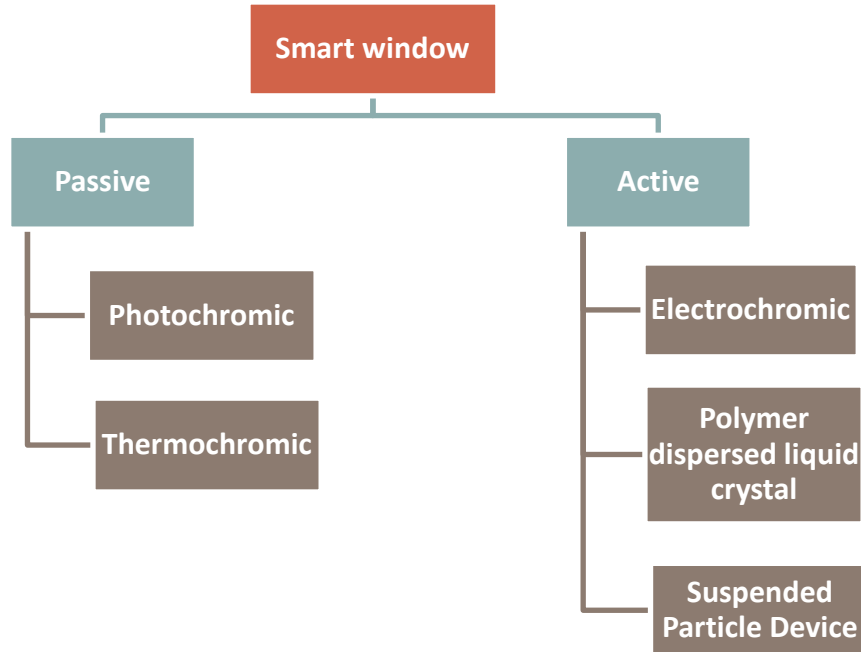


Figure 3 Classification of smart window technologies.

Electrochromic windows have gained a lot of attention as they allow the user to control their operation to meet personal preferences. It allows the users to control the amount of heat or light that passes through the glass. Such windows use materials that undergo a change in color or opacity in response to electricity. Requirement of power supply complicates the design of such windows leading to complexities in installation. Upgrading static windows in current buildings to electrochromic windows can be a complicated and expensive task.

Thermochromic windows have gained attention due to their low fabrication and maintenance cost and ease of installation in new as well as existing systems. Thermochromic windows use thermo-responsive materials that passively undergo a change transmittance in response to the temperature they are exposed to. The most common configuration (shown in figure 4) of a thermochromic window is a double pane glass with the thermo-responsive material sandwiched between the two glass substrates. Such windows switch between transparent and opaque states at a specific temperature ( $T_c$ ). At temperatures below  $T_c$ , the window is designed to be transparent. At temperatures above  $T_c$ , the window changes to an opaque state. The main objective behind designing thermochromic windows is to control and tune the transition temperature of the thermo-responsive polymer to bring it closer to an ideal indoor temperature for comfort and efficiency.

Secondary objectives include increasing durability and increasing the contrast between the transparent and opaque states to optimize the modulation of solar energy.<sup>9</sup> Multiple requirements need to be fulfilled for incorporating thermo-responsive materials into windows commercially<sup>10–13</sup>.

- Temperature dependent switching should take place between clear and opaque states, with transmittance in clear state  $>85\%$  and  $<15\%$  in opaque state.
- Transition temperature tunable over a wide range that can be adapted to climatic and architectural needs.
- Opacity of the material should change homogenously over the entire area without any streaking.
- The transition must be reversible and reproducible over a long period of time.
- All components of the system should be harmless, non-flammable, biologically degradable.
- Low-cost material.

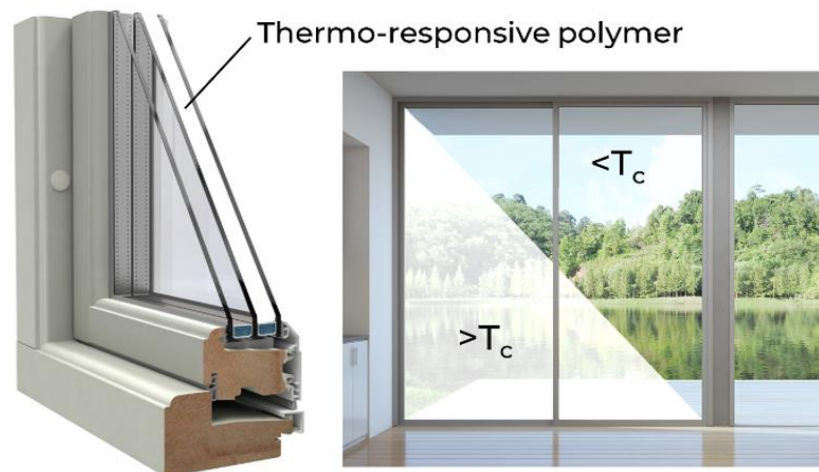


Figure 4 Typical configuration of thermochromic windows

There are multiple ways of installing a smart window in a space 1) Completely removing and discarding the existing window in a space and replacing it with a smart window 2) Simply adding an additional layer or modifying the existing window. The latter process is referred to as retrofitting. Though the former approach is more comprehensive, it involves a high upfront cost



and significant time and energy. The latter approach is much simpler, cost effective and requires lower amount of cost and energy. This makes retrofitting an attractive option for renewing older building technologies to make them more energy efficient.

The quality of the window is judged by its insulating value and its transparency to sun's visible and infrared light. The part of the electromagnetic spectra that reaches the earth is between 100 nm and 1mm. This band consists of three ranges: the ultraviolet visible and infrared radiation. The ultraviolet region lies between 100-400nm. The visible light falls between 400-700 nm. These are the only radiations that are visible to the human eye. The infrared region lies between 700nm to 1mm. The infrared radiation are responsible for warming up the surface of earth. An ideal window should provide optimum lighting level without glare, high level of thermal insulation and allow the infrared light to pass when it is useful for heating but block it when it adds to the cooling load.<sup>7</sup> It should block the ultraviolet light that can lead to skin and material damage.

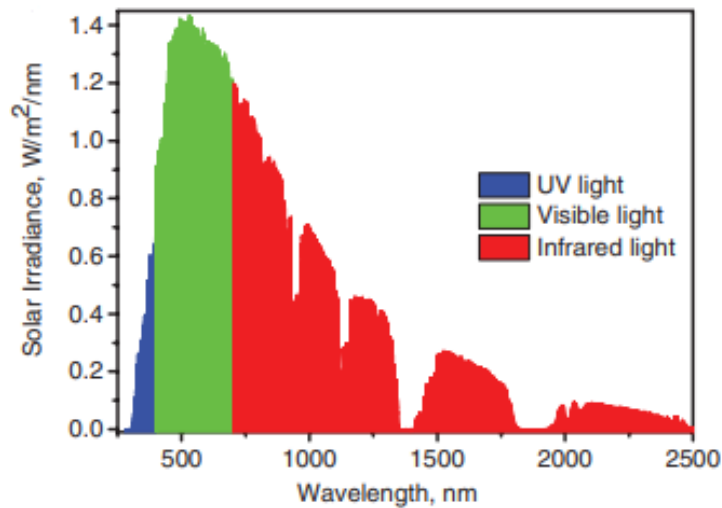


Figure 5 Solar Spectrum on Earth

Despite their numerous advantages, market penetration of smart windows has been slow. Perhaps the most important reason is the cost associated. Smart windows are high performance, architected windows that can add significantly to the cost. Smart windows are usually sold at a higher cost as compared to normal windows.<sup>9</sup> Another reason behind the resistance to adoption of smart windows can be the complexity of their integration into homes. Various user related considerations such as transition temperature, color of darkened state, requirement of power

sources and complexity of installation contribute to the decision of installation of smart windows. Such complexities can lead to frustration among users, and in turn discourage market entry. In this thesis, we explore the use of a cellulose based thermochromic smart window that has the potential to address these concerns.

This thesis focuses on the use of cellulose-based hydrogels in thermochromic windows, coupling the numerous advantages of cellulose with its thermo-responsive behavior. These features alongside the abundant availability of cellulose couples with the low cost associated with manufacturing of cellulose derivatives makes cellulose-based hydrogels particularly attractive candidate for smart window application.

### **1.3 Outline of Thesis**

Chapter 1 introduces the reader to the building energy consumption trends in the U.S., smart window technologies, advances in thermochromic smart window technologies and advantages of thermochromic smart window technology. Advantages of hydrogel based thermochromic smart windows are discussed and compared to other researched thermochromic materials. The literature review goes over the published studies associated with smart window technologies.

Chapter 2 discusses the material system of the thermochromic window. The structure and applications of cellulose is introduced. Further discussion has been focused on Methyl Cellulose. The structure, solution thermodynamics, gelation mechanism, LCST tunability and applications of MC have been studied.

Chapter 3 discusses the experimental method and basic principle of characterization techniques. It outlines the sample preparation techniques and procedures for characterization.

Chapter 4 discusses the results from the characterization. It discusses results from the tests for transition temperature measurements, effects of salts on the transition temperature, spectroscopy measurements for transmittance in the visible range, freeze resistance and a model demonstration.

Chapter 5 draws together the study by summarizing the results and suggesting a future research direction.

## 1.4 Literature Review

One of the major driving forces behind the research interest in smart window technologies in the industrial and academic community is the large business market. The size of the global market for smart windows was valued at USD 3.8 billion in 2020 and is estimated to reach USD 6.8 billion in 2025 with an annual growth rate of 12.1%.<sup>14</sup> Thus, there has been a rise in investments in smart window technologies targeting occupant comfort and energy saving.<sup>15,16</sup>

Owing to the huge progress in the field of material science, many new technologies for smart windows based on different stimuli are entering the market. The fundamental mechanism of smart windows is based on their tunable optical transmittance which is generally promoted in response to an applied bias or changing environmental conditions. This review systematically investigated the published research associated with smart window technologies. This review will consist of the following sections 1) an overview of the existing smart window technologies 2) a review of thermochromic windows 3) a review of cellulose hydrogels.

### 1.4.1 Smart window technologies

Smart window technology has undergone rapid development based on source of the required stimuli. Research has been focused on windows based on electro-, photo-, thermo-responses. Among all these, electrochromic windows have undergone gradual evolution in the span of many years and several electrochromic windows are commercially available in the market today.<sup>17–20</sup> Mechano-chromic windows rely upon materials that display reversible structural changes in response to external strains.

Traditional active smart window technologies are based on electrochromic materials, suspended particles or polymer dispersed liquid crystal materials.<sup>21</sup> An electrochromic glass modulates the light transmission and solar radiation by sending an electric charge through the glass. The glass darkens or lightens when voltage is applied to the system. An electrochromic window consists of five layers of materials sandwiched between the two glass substrates of a double pane window.<sup>22</sup> It consists of two transparent conducting oxide layers surrounding an electron accumulator, an ion conductor layer and an electrode layer. Despite its advantages, market adoption of electrochromic glass has been slow. Due to complexities in construction, electrochromic glass can cost around \$100/m<sup>2</sup>.<sup>23</sup> Functioning of electrochromic windows require

a constant supply of electricity which can add to the energy consumption of the building. Being an active system, the installation and maintenance of such windows can be complicated and expensive. Many researchers have investigated windows based on liquid crystal technologies. However, a major drawback in their widespread application is the cost associated with manufacturing of liquid crystals.<sup>24,25</sup>

Passive systems function autonomously in response to natural stimuli such as light (photochromic window), gas (gasochromic window) and heat (thermochromic window). This leads to an easy installation and good reliability of the system.<sup>26</sup> Photochromic materials show a reversible change color when exposed to certain wavelengths of light. Photochromic windows have an easy construction and do not require an energy input for operation. Photochromism is the reversible transformation of a specimen between two states by the absorption of electromagnetic radiation. The two said states have a different absorption spectra.<sup>27</sup> Photochromic materials undergo a structural transition between two chemical isomers having different absorption spectra. During the transformation of molecule between its isomer states, the rearrangement of chemical bonds leads to structural and electronic changes. All photochromic materials experience a colorization on UV irradiation. However, the color of the organic photochromic material cannot be switched back simply by removing the UV source. Such a challenge restricts the application of organic photochromic materials as smart windows. Inorganic photochromic materials are able to change their color on removing the UV light. Thus, the color of inorganic photochromic materials can be easily controlled.<sup>28</sup>

Table 2 Comparison of Thermo-, Electro-, and Photo- chromic windows<sup>28</sup>

	<b><i>Thermo-chromic</i></b>	<b><i>Electro-chromic</i></b>	<b><i>Photo-chromic</i></b>
<i>Actuation</i>	Passive	Active	Passive
<i>Stimuli</i>	Thermal	Electrical	UV light
<i>Device complexity</i>	Low Simple coating or encapsulation	High Multilayered structure with electrical control system requirement	Low Simple coating or encapsulation
<i>Energy Saving Potential</i>	Suitable	Suitable, with a one-time low energy input	Suitable for tropical countries
<i>Optical transition speed</i>	Acceptable	Acceptable	Acceptable

Table 2 gives a brief comparison between the four major categories of smart windows. Though some smart window technologies have been commercialized<sup>17–20</sup>, some technical and economical hurdles prevent their market adoption.

#### 1.4.2 Thermochromic windows

Thermochromism is a property of materials, what results in a temperature induced change in transmittance and optical properties. Once the temperature is over the transition temperature (or LCST), the material will modulate transmittance of light by switching from a high transmittance (clear) state to a low transmittance (opaque) state autonomously. Thermochromic materials have a lot of potential in technological applications such as smart windows, passive radiators temperature sensors and camouflage devices.

Thermo-responsive polymers undergo a temperature dependent sol-gel transition. Based on their response to temperature, such polymers can be classified into two categories; first, polymers that undergo a phase change above the critical temperature called Lower Critical Solution Temperature (LCST) and second category of polymer that undergo a phase change below a critical temperature called as the Upper Critical Solution Temperature (UCST). Thermo-responsive polymers dissolved in aqueous systems having a lower critical solution temperature (LCST) are miscible at normal temperature, but their solubility decreases as the temperature is

increased, and above a critical temperature or a transition temperature (LCST) they show phase separation. For polymers showing USCT, they remain miscible above the critical temperature (USCT) and phase separation occurs when the temperature falls below the critical value.

In recent times, smart windows based on thermo-responsive materials are gaining attention because of their autonomous operation without the requirement of a power input and low cost, resulting from simple design, inexpensive maintenance, and ease of retrofitting. Thermochromic windows have been referred to as “smart”, “switchable”<sup>9,29</sup> or “intelligent”<sup>13,30,31</sup> windows. “Smart” refers to the ability of such windows to autonomously modulate solar transmittance when triggered by temperature. Traditionally, many studies about thermochromic smart windows have been focused on Vanadium Oxide ( $VO_2$ ).<sup>3,32</sup> Vanadium Oxide based smart windows adjust the transparency of a window in response to temperature, without the requirement of a power source. However, the applications of  $VO_2$  based smart windows are limited by their various shortcomings.  $VO_2$  has a high transition temperature ( $\sim 68^\circ C$ ) at which it drastically lowers its transmittance in infrared region and experiences only a negligible change in the visible range.<sup>3</sup> It gains a black tint at the transition temperature which is unattractive and undesirable.<sup>33</sup>

Metamaterials are also considered as potential candidates for smart window applications.<sup>3,34</sup> Metamaterials are temperature responsive reconfigurable structures, whose properties arise from dynamically tunable geometric structures rather than composition. Thermochromism for smart windows using metamaterials was achieved using origami inspired structure. Such structures respond environmental temperature change by changing the metamaterial configuration.<sup>3</sup> Thermo-responsive origami structures, called kirigami, have been examined for thermochromic smart window application.<sup>34</sup> Such structure either reflect or transmit light in response to changing ambient temperature by buckling out of plane. This structure consists of notches that change their orientation by tilting at angles that either reflect or transmit light. However, current experiments have evaluated the performance of metamaterials at macro-scale. It is important to study the performance of such materials at micro and nano scale.

Thermochromic hydrogels make excellent materials for application in smart window technologies. Hydrogels consists of hydrophilic polymer chains that possess a three dimensional network.<sup>35,36</sup> They are hydrophilic crosslinked polymers that exhibit a considerable water swelling capacity.<sup>37</sup> Due to its swelling properties, hydrogels have the capability of including other molecular species in their structure. Thus, hydrogels find immense applications in the medical and

pharmaceutical industry because of their ability to carry therapeutic agents like peptides and proteins in their structure. Certain hydrogels are stimuli responsive substances that respond to external stimuli such as temperature, pH, electric field, or other chemical stimuli. Thermochromic hydrogels are transparent to light at low temperatures, while they strongly scatter the incident light at higher temperatures as a result of formation of polymer aggregates which serve as scattering centers for light.<sup>3</sup>

To address this issue related to  $VO_2$  and metamaterials based smart windows, studies have been focused on temperature responsive hydrogels including poly-ampholyte hydrogel (PAH)<sup>38</sup>, poly(N-isopropylacrylamide) (PNIPAm)<sup>30,36,37,39</sup> and Hydroxypropyl Cellulose (HPC).<sup>40</sup> Majority of such polymers possess a Lower Critical Solution Temperature (LCST), above which the polymer becomes insoluble. Consequently, the polymer switches between transparent and opaque states on heating and cooling.<sup>39</sup> These polymers allow the incident light to pass at low temperature, and strongly scatter the incident light at higher temperatures due to formation of aggregated polymer nanoparticles which act as scattering centers.<sup>36</sup> This LCST characteristic makes thermo-responsive polymers promising candidates for energy efficient smart windows. By limiting the transmission of solar radiation through the window, the indoor temperature can be reduced, in turn limiting the use of energy for air conditioning.

Poly(N-isopropylacrylamide) (PNIPAAm) is a thermo-responsive polymer that has a variety of applications in tissue engineering, drug delivery and smart windows based thermochromic windows<sup>30,37,39,41</sup> have been reported to have an LCST~ 32°C.<sup>39</sup> At temperatures below the LCST, PNIPAAm is transparent. At this state, the hydrogel is in a homogenous state with the polymer chains caged by water molecules, held together via hydrogen bonding. Once the temperature is increased above LCST, the intramolecular hydrogen bonds begin to break, and formation intermolecular hydrogen bonds leads to phase separation of the PNIPAAm hydrogel. The phase separation results in the change in optical state of the hydrogel. It was observed that optical transmission spectra of a PNIPAAm based thermochromic smart windows varies with changing polymer thickness.<sup>42</sup> Even though PNIPAAm has a lower LCST that is desirable for smart window application, it has a few limitations. PNIPAm hydrogels require perfectly sealed glazing systems. If not sealed properly, the hydrogel layers dries out, losing its reversible thermo-responsive behavior.<sup>39</sup> PNIPAAm is limited by its complicated fabrication process difficulty in

removing its odor.<sup>41</sup> PNIPAAm based smart windows have a poor freeze resistance, which decreases the transmittance at low temperatures.

### 1.4.3 Cellulose hydrogels

Researchers are focusing their attention towards green and renewable concepts as an important part of every research to develop and apply environmentally friendly products using natural raw materials. The use of bio-based materials as renewable resources in various applications to help mitigate environmental issues. Thus, cellulose is becoming a preferred candidate to displace fossil-based materials.<sup>43</sup> Cellulose is a compound of interest in various applications because of its natural and renewable origin, abundance and properties that make it a material with a wide range of applications. Cellulose can be used to fabricate functional materials that present intelligent behavior when exposed to certain environmental stimuli. Many studies have been focused on the thermo responsive properties of cellulose due to its many outstanding merits such as being inexpensive, non-toxic, biocompatible and biodegradable.<sup>13,41,42,44</sup>

As discussed in previous section, hydrogels are high porosity, macromolecular networks that can hold large amount of water. Potential applications of hydrogels are in the field of food, biomaterials, agriculture, water purification, etc.<sup>45</sup> Recently, researches have been exploring the potential applications of hydrogels in tissue engineering<sup>46,47</sup>, drug delivery<sup>35,48,49</sup>, contact lenses<sup>50</sup>, sensors<sup>51</sup>, purification<sup>52</sup>, etc. Cellulose hydrogels have many attractive properties such as hydrophilicity, biodegradability, biocompatibility, transparency, low cost and non-toxicity. Cellulose based hydrogels are formed by crosslinking aqueous solutions of cellulose ethers such as methyl cellulose (MC), ethyl cellulose (EC), hydroxyethyl cellulose (HEC), which are among the most widely used cellulose derivatives.<sup>40</sup> Various water soluble derivatives can be used independently or in combination to form a hydrogel. The smart behaviors of some cellulose derivatives in response to physiological variables such as pH, ionic strength, temperature, makes the resulting hydrogel appealing options for in vivo applications.<sup>53</sup>

Superabsorbent Polymer (SAP) are used in personal care products. Such polymers are commonly used in diapers to keep skin dry and prevent rash. Acrylate based SAPs pose environmental concerns due to non-biodegradable nature.<sup>53</sup> Cellulose based hydrogels based on carboxymethyl cellulose (NaCMC) and hydroxyethyl cellulose (HEC) are being studied as they possess capabilities comparable to the SAPs and can address the issue of biodegradability and



recycling.<sup>53</sup> Superabsorbent hydrogels are also being used in agriculture to optimize the water resources in agriculture and horticulture. Swollen hydrogels can release water and added nutrients slowly through a diffusion-driven mechanism when there is a humidity differential inside and outside of the material. Hydrogels have also been used in the development of wound dressings, either as sheets or amorphous form. Due to its purity and high-water retention capacity, bacterial cellulose (BC) has been investigated for wound healing and dressing. Temperature sensitive cellulose ethers also find applications in the pharmaceutical industry for drug delivery formulations. Such hydrogels have the ability to swell and de-swell as a result of changing temperature of the surrounding temperature. Cellulose based hydrogel tablet have been developed that result in a controlled release of drugs in the body due to their swelling properties.<sup>53</sup> Temperature sensitive polymers are also known as thermo-responsive materials. Such hydrogels exhibit a phase separation above a certain temperature. This phase change results in a sol-gel transition with the gel state being opaque. This behavior of thermo-responsive polymer makes it an ideal candidate for thermochromic windows.

## **2. THERMOCHROMIC SMART WINDOWS**

With the aim of tackling climate change, resource shortages and waste disposal issues, researchers are focusing their attention towards developing environmentally friendly and renewable material alternatives for various technologies. Chemically modified polymers are being actively investigated to develop newer materials.

### **2.1 Cellulose**

Cellulose is the most abundant, sustainable, renewable, and biodegradable organic material present in the biosphere. It is present in the cell walls of plants, algae, and shells of tunicates. Cellulose is widely used in the industry for applications such as making paper and paper products, biofuel, gunpowder, etc. Approximately  $5 \times 10^{11}$  metric tons of cellulose is generated every year.<sup>54</sup> It is a colorless, odorless and nontoxic substance. It is a linear homopolymer polysaccharide that is insoluble in water. Cellulose consists of multiple D-glucose subunits linked together. These glucose units are linked via 1-4 glycosidic bond. Every alternate glucose molecule in the cellulose chain is inverted. Multiple such chains are arranged parallel to form microfibrils. Such arrangement of cellulose chains gives it a great mechanical strength. Pure cellulose is odorless, hydrophilic, insoluble in water, and biodegradable. Thus, cellulose is applied to a vast array of fields. Thus, cellulose provides a green, efficient, non-toxic, and affordable solution.

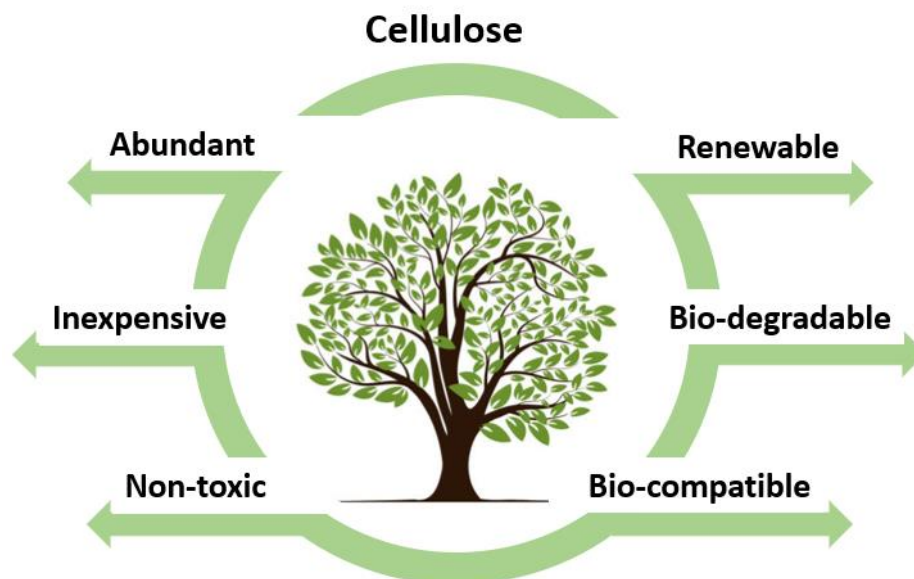


Figure 6 Advantages of cellulose

Unlike fossil-fuel based products, our forest resources are renewable. By proper management of forest resources, wood products can be maintained indefinitely.<sup>55</sup> It is hard to emphasize the importance of wood based products on our economy and standard of living. Sustainability of this reserve depends on the forestry and harvesting practices. The sustainability of forests can be managed by maintaining the forest's productivity, biodiversity and regeneration capacity while ensuring that they can meet the society's needs now and in the future. A good sustainable forest practice imitates nature's patterns of destruction and regeneration, while balancing the requirements of the environment, wildlife, forest communities while conserving trees for generations to come.<sup>56</sup> Harvesting cellulose as a part of forest management program can not only avoid deforestation for obtaining cellulose but also can help maintain the health of the forest. Proper forest management can help avoid droughts, insect attacks and forest fires. Overcrowding of trees in forest can result in the trees competing for light, water, and other resources. This stress can lead to droughts and insect attacks. Removing some trees can ease the competition and allow the trees to grow bigger and healthier. Such activities need careful study and planning.

Powdered cellulose is obtained by the purification and size reduction of cellulose obtained from pulp from fibrous plant materials. Cellulose is derived from wood fiber and is refined to varying degrees based on its application. Commercially, the raw material used for manufacturing

cellulose powder is wood. Logs of wood are obtained and passed through a wood chipper to transform the wood into pellets. These pellets are fed into a digester to separate the lignin from the fiber of the tree. The wood chips are cooked in presence of sulfurous acid and sulfur dioxide to dissolve the lignin. Certain applications demand the cellulose to be bleached to remove any brown pigment left behind by lignin. In the final step, the cellulose is sieved and washed to remove sand particles and is adjusted to the specified size distribution. At the end, a white, odorless and tasteless powder of varying particle sizes is obtained.

Despite the great potential of cellulose, it is insoluble in water due to its strong inter and intra molecular hydrogen bonds, which lead to the formation of its crystalline structure. To overcome this challenge, cellulose derivatives are obtained by substituting the  $-OH$  groups by  $-OR$  groups, which lead to a variety of cellulose derivatives. Cellulose is available in the market in different forms with varying properties. The difference in properties of forms of cellulose is depends on the shape, size and degree of crystallinity of their particles. Cellulose ethers and esters are the two broad groups of cellulose derivatives which possess different chemical and mechanical properties. Cellulose ethers are produced by replacing the hydrogen atoms in the hydroxyl groups in the anhydro glucose units of cellulose with alkyl or substitutes alkyl groups. Cellulose esters are obtained by replacing the hydrogen atom in the hydroxyl group by acid residues.<sup>57</sup> The degree of substitution gives the number of hydroxyl groups that have been substituted in a glucose unit. The degree of substitution can be controlled to a certain extent to obtain derivatives with the desired solubility and viscosity in water solution. Methyl Cellulose (MC), Hydroxypropyl Cellulose (HPC), Hydroxypropyl Methyl Cellulose (HPMC) and Carboxymethyl Cellulose (CMC) are among the most exploited cellulose derivatives, not only due to their water solubility but also because of their functional nature. CMC produces a pH responsive hydrogel, whereas MC, HPC and HPMC produce temperature responsive hydrogels.<sup>40</sup>

Hydrogels are high porosity, macromolecular networks that can accommodate large amount of water. Upon contact with water, hydrogels absorb water and swell to form 3D structures due to the presence of hydrophilic groups such as  $-NH_2$ ,  $-OH$ ,  $-COOH$ ,  $-SO_3H$  in the polymer network. The ability of the polymer to hold the 3D structure is due to physical and chemical crosslinking that also prevents the hydrogel from dissolving in the solvent. Hydrogels based on natural cellulose can be prepared from pure cellulose solution through physical crosslinking due to hydrogen bonding between hydroxyl groups on the cellulose chains.

In this work, we introduce and utilize a methyl cellulose based thermochromic smart window, which is scalable, biocompatible, and has great potential for commercialization. Some derivatives of cellulose prepared by etherification become water soluble and show thermo-responsive gelation.<sup>40</sup> Thermo-responsive gelation refers to the sol-gel transition of the polymer in response to temperature stimulus. The temperature at which gelation occurs is known as Lower Critical Solution Temperature (LCST). This phase separation is controlled by the balance between hydrophilic and hydrophobic groups on the polymer chain.<sup>40</sup>

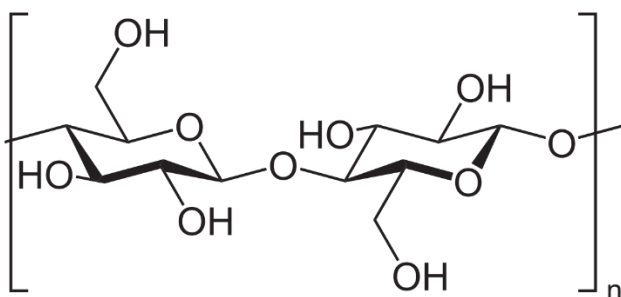


Figure 7 Structure of Cellulose

## 2.2 Methyl Cellulose structure

Methyl Cellulose is one of the most important cellulose derivative as it has been utilized in various industrial applications.<sup>58</sup> Methyl Cellulose is a methyl ether of cellulose produced by partially functionalizing the cellulose backbone with methyl groups. In methyl cellulose,  $-OH$  groups in the cellulose chains are substituted with methoxy groups  $-OCH_3$  groups. Hydroxyl groups at C-2, C-3 and/or C-6 position in a cellulose backbone are substituted by methyl groups ( $-CH_3$ ) to derive MC from cellulose. MC can be prepared via two ways: a homogenous preparation allows uniform distribution of the methoxy groups on the cellulose macromolecule. Heterogenous preparation produces cellulose macromolecules with random distribution of the methoxy groups. Commercially Methyl Cellulose is produced in the heterogenous way, using a two-step reaction. First the cellulose is exposed to sodium hydroxide which results in an alkali-cellulose product. In the second step this product is treated with methyl chloride to obtain methyl cellulose. Regions rich in  $NaOH$  result in rapid methylation which results in a heterogenous distribution of methoxy groups on the cellulose macromolecule.<sup>59</sup>

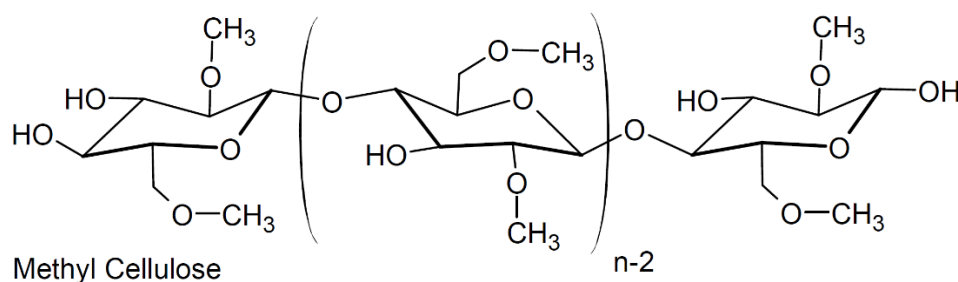


Figure 8 Structure of Methy Cellulose

Pure cellulose is not water soluble because of its strong intermolecular hydrogen bonds. Some of these hydrogen bonds are broken when certain number of hydroxyl groups are substituted with methyl groups.<sup>60</sup> Thus, methyl cellulose has improved water solubility properties as compared to pure cellulose. To ensure desired water solubility, the Degree of Substitution (DS) should be controlled. Methyl Cellulose consists of about 27-32% of the hydroxyl groups substituted in the methyl ether form.<sup>40</sup> For a heterogeneously produced MC, water solubility has been observed for a  $DS > 1.3$ .<sup>59</sup>

### 2.3 Methyl Cellulose applications

Methyl cellulose is gaining traction in the global market and is expected to experience an upward graph of revenues during the forecast period between 2020 and 2030. Methyl Cellulose is gaining interest in various sectors such as construction, cosmetic and personal care, food additives, paints and coatings and pharmaceutical. The key reason for the popularity of Methyl Cellulose is its non-allergic and non-irritating nature.

MC is food grade and is widely accepted in food applications by many countries in the world. Like cellulose, it is non-digestible, non-toxic and non-allergic. It is used as an emulsifier which prevents separation of two mixed liquids. It is also used as a thickener and a gelling agent. As it cannot be digested or absorbed, it serves as a calorie-free material. It is often used to improve texture and increase volume of in bakery products. MC is commonly used in ice-creams as to reduces the growth of ice-crystals during freezing. MC is used to control the viscosity and emulsion stability of creams, dressings and sauces.

It is often also used in cosmetics and personal care products as it is regarded as nontoxic, nonallergenic and nonirritant material.<sup>61</sup> It is added to hair shampoos, hair styling products, liquid soaps, lotions and creams to generate a thick consistency.

MC is used in a variety of oral and topical pharmaceutical products. As MC is not digestible, it is used as an additive in the pharmaceutical industry. It is also used to manufacture capsules for nutritional supplements. As MC is not absorbed in the intestine, it can pass through the digestive track undisturbed. As it can absorb large amounts of water into the colon. It aids with the treatment of constipation and irritable bowel syndrome. Thus, it is often used as a laxative.

MC also finds applications in construction materials. When added to mortar dry mix, it improves properties of the mortar such as workability, water retention, viscosity and surface adhesion.<sup>62</sup> Such mortars include tile adhesives, insulating plasters, skim coats, joint and crack fillers, etc. MC is also used to modify the rheological properties of paint to prevent it from sagging. MC is also used as a weak adhesive in many applications such as binding books, fixing delicate art pieces, making wallpaper pastes, etc.

MC is used in agriculture as a dispersing agent for wettable pesticide and fertilizer powder. It enhances the adhesion of the pesticides and nutrients to plant surfaces.<sup>62</sup>

## **2.4 Methyl Cellulose Gelation Mechanism**

MC hydrogels that are prepared from aqueous solutions of Methyl cellulose display a thermo-responsive behavior. Aqueous solutions of Methyl Cellulose when heated undergo a reversible sol-gel transition at a temperature characteristic to its concentration. In the sol state the polymer chains are free to move in the solvent, while the state in which the polymer chains bind together forming an interconnected network is called the gel state. The temperature at which the molecular arrangement changes from a sol state to a gel state is called the lower critical solution temperature (LCST). The sol-gel transition results in a change in the turbidity of the solution. The gelation mechanism of Methyl cellulose has been studied extensively and various gelation mechanisms have been reported.<sup>60,63–69</sup> The sol-gel transition of MC has been illustrated in Figure 10. Black solid lines represent cellulose chains with short branches as methoxy groups. Blue dots represent water molecules. The illustration shows two cases: 1. Low MC concentration (top) 2. High MC concentration (bottom). At low temperatures (temperatures below LCST), water molecules surround the hydrophobic methoxy groups due to their polar nature. Water molecules

form hydrogen bonds along MC chain forming a cage like structure around the MC chain resulting in MC becoming water soluble. Heating of the MC solution causes the hydrogen bonds to break and destructs the cage structure around the MC chain. This exposes the hydrophobic regions of the MC chains, leading to the formation of hydrophobic aggregates. As the temperature keeps increasing, the number and size of these hydrophobic aggregates increases leading to the formation of a gel.<sup>63</sup> The association of hydrophobic groups leads to the formation of a three-dimensional network of MC chains.<sup>63</sup> Water molecules get trapped in the network leading to a flexible gel structure. Upon cooling the polymer to a temperature below LCST, the dissociation of the hydrophobic interactions leads to the loss of the gel structure of MC and reverses to the sol state. The aggregated polymer clusters reduce the transparency of the hydrogel by scattering incident light.<sup>3</sup> This transition from the sol-gel state is reversible due to the non-covalent nature of the chemical interactions involved in the process.

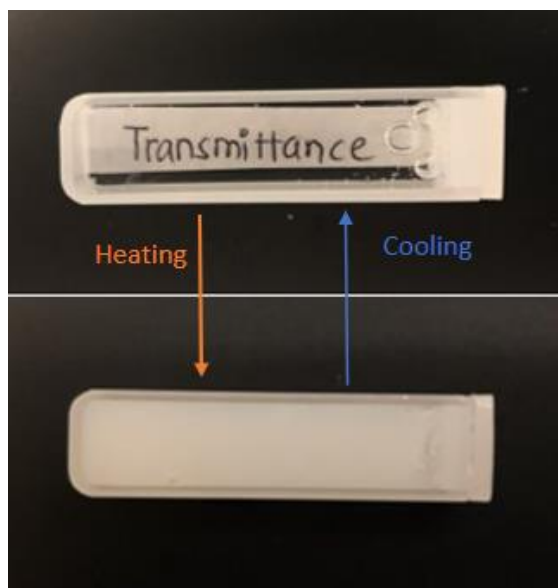


Figure 9 Clear and Opaque states of a MC aqueous solution

## 2.5 Methyl Cellulose solution thermodynamics

It has been previously reported that the sol-gel transition of MC is an endothermic process.<sup>60,70</sup> As discussed previously, the sol-gel transition of MC is a result of microscopic phase separation caused by the destruction of cage like structure and formation of hydrophobic associations between methyl groups. The amount of energy required for the formation of



hydrophobic associations is greater as compared to the amount of heat absorbed while breaking the water cages.

For a process to be thermodynamically feasible, it is required that the Gibbs free energy ( $\Delta G$ ) for the process to be negative. ( $\Delta G = \Delta H - T \cdot \Delta S < 0$ ). For polymer exhibiting LCST behavior, the Gibbs free energy is negative at temperatures below LCST, when the polymers tend to dissolve in the aqueous system. When a polymer is dissolved in a solvent, variety of interactions between the polymer and solvent are involved in the process. If  $\Delta H$  is positive,  $\Delta S$  must also be positive to meet the requirement of negative Gibbs energy change. It has been previously reported that the sol-gel transition of MC is dictated by entropy change rather than enthalpy change.<sup>60</sup> The entropy change of the sol-gel transition can be explained by the entropy contribution of water. The hydration layer formed by water around the hydrophobic methyl group have an ordered cage like structure. As the temperature of the MC solution is increased, the water cages break, and the water molecules become free. The entropy of the system increases. The hydrophobic units associate to form hydrophobic aggregates. Thus, during sol-gel transition the water molecules go from a relatively ordered state to a random state, resulting in a positive  $\Delta S$ . The positive entropy ( $\Delta S$ ) is able to overcome the positive enthalpy ( $\Delta H$ ) value, and a negative ( $\Delta G$ )

## **2.6 Methyl Cellulose LCST tunability**

The LCST of MC hydrogels can be tuned by acting on multiple factors i) MC degree of substitution ii) MC concentration iii) anions, etc. These factors should be chosen depending on the final envisaged application.

### **2.6.1 Degree of Substitution**

The LCST or transition temperature of MC depends on the balance between the hydrophilic and hydrophobic groups in the MC solution. As mentioned earlier, this ratio can be controlled by controlling the degree of substitution of MC, i.e., controlling the number of methoxy groups substituted on the cellulose chain. Thus, the LCST can be reduced by increasing the DS. It has been previously reported that increasing the number of methoxy group substitutes promotes hydrophobic associations at lower temperatures.<sup>70–72</sup> However, to maintain the water solubility of MC in water, the DS should be maintained in the range 1.3–2.5.<sup>73</sup>

### **2.6.2 Methyl Cellulose concentration**

The gelation temperature of the MC solution can be controlled by varying the concentration of MC in the solution. At low MC concentrations, almost all the MC molecules are linked to water molecules via hydrogen bonding. Lesser number of hydrogen bonds between the MC chains at low MC concentrations result in higher transition temperatures. At higher concentrations of MC, the solution will have a higher concentration of the hydrophobic methyl groups, and a weaker water cage structure around it. Thus, the energy required to break the hydrogen bonds is lower, resulting in a lower transition temperature. Thus, as the concentration of MC has an inverse relation with the gelation temperature. This can be seen in the schematic shown in figure 10.

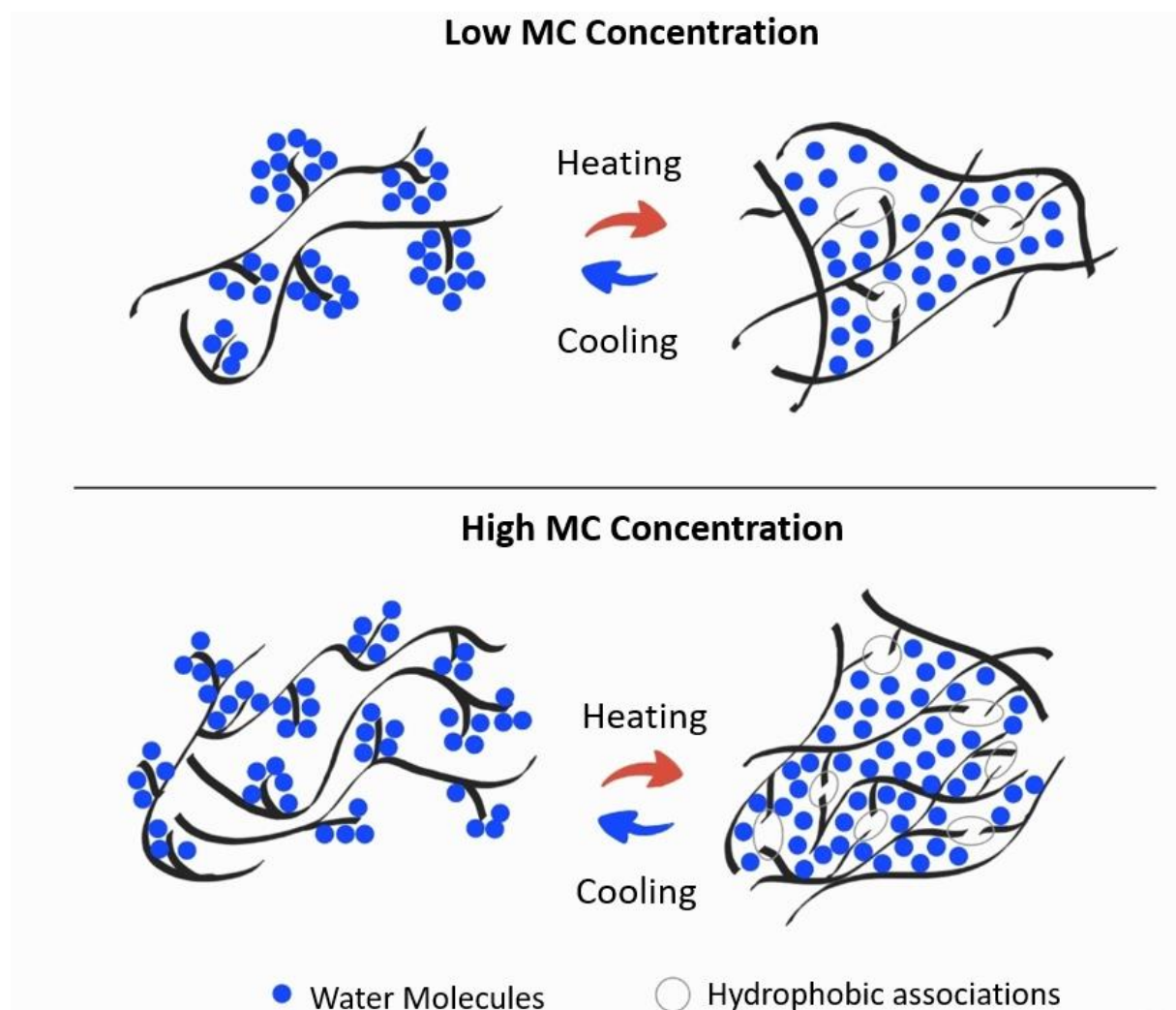


Figure 10 Gelation mechanism of MC solution for low (top) and high (bottom) concentrations of MC. Part (a) shows state of MC chains at temperature below the LCST of cellulose. (b) shows temperatures higher than LCST.

### 2.6.3 Anions

Ions in the form of organic salts have been reported to tune the transition temperature of thermo-responsive polymers.<sup>60,69,74,75</sup> Franz Hofmeister first studied the effect of ion on the solubility of a polymer in 1888 when he studied the solubility of proteins in an aqueous solution. Hofmeister ions in the form of certain salts have the ability to precipitate certain proteins out of an aqueous solution. Even though the series has been used to study the denaturing of proteins, it has

been applied in many fields of science. It has been observed that the Hofmeister ions exhibit these effects on polymers as well.<sup>60,63,69,75–77</sup>

It has been previously reported that salts can have a significant effect on the phase behavior of water-soluble polymers. Most inorganic salts decrease the solubility of the solute, whereas some increase solubility of the solute.<sup>60</sup> These effects are called salting-out and salting-in, respectively. The Hofmeister series ranks the ions in terms of how strongly they affect the hydrophobicity. According to the Hofmeister's series, ions can either behave as kosmotropes (structure makers) or chaotropes (structure breakers). Kosmotropes and chaotropes refer to the ability of the ion to stabilize and weaken the structure of water respectively. A typical Hofmeister order for anions is shown in the figure 11.

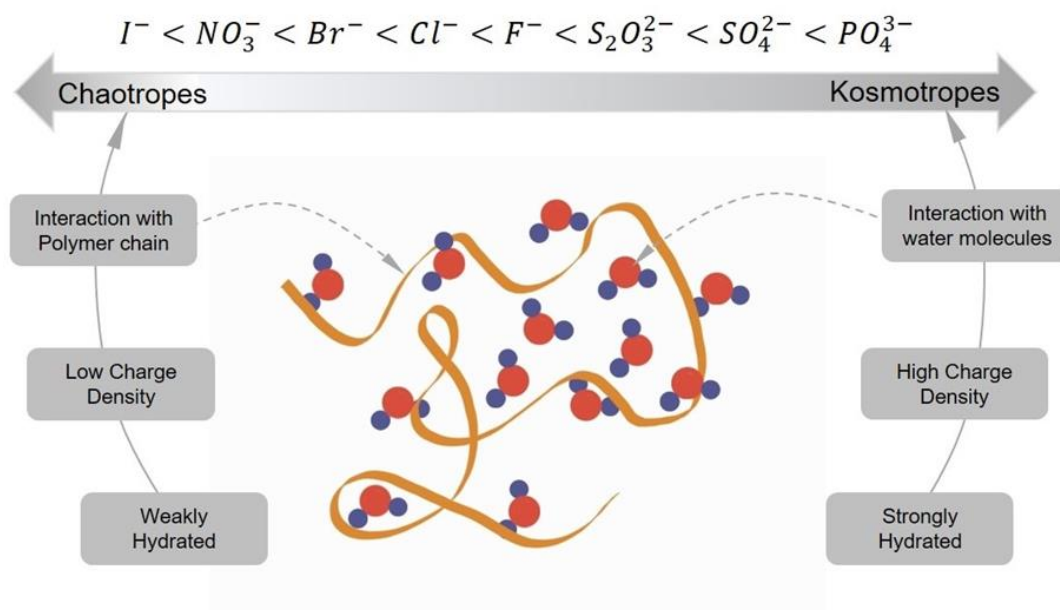


Figure 11 Hofmeister series: ions on the left producing a salting in (stabilizing) effect on the polymer, whereas ions on right lead to salting out (destabilizing) effect

The effect of different ions on the stability of the thermo-responsive polymer can be quantified by the change in the transition temperature of the thermo-responsive polymer as a function of the type of salt and its concentration. As seen from the figure 11, the ions to the right of the series are called kosmotropes. These ions strongly bond with the water molecules in the solution and enhance the stability of the polymer. Thus, kosmotropes enhance the hydrophobicity

of a solute, or cause “salting out”. This results in a decrease in the transition temperature. Ions towards the left of the series, called chaotropes, exhibit a strong destabilizing effect on the polymer in the solution. Chaotropes increase the solubility of a non-polar solute, or cause “sating in”. This results in an increased transition temperature.

### 3. EXPERIMENTAL METHODS

This chapter discusses the sample preparation and characterization techniques. It informs the reader of the procedures followed for the experimental characterizations.

#### 3.1 Materials

Methyl Cellulose ( $M_w \approx 88\,000\text{ g/mol}$ , Sigma-Aldrich) was used as the thermo responsive polymer. It consists of cellulose with methoxy substitution between 27.5-31.5% and a Degree of Substitution (D.S., average number of substituent groups attached to the ring hydroxyls) between 1.5-1.9. The powder was used as received without further purification.

Analytical grade Sodium Phosphate ( $Na_2PO_4$ ), Sodium Chloride ( $NaCl$ ) were obtained from Sigma Aldrich. Analytical grade Sodium Sulphate ( $Na_2SO_4$ ), Sodium Fluoride ( $NaF$ ) was obtained from Fisher Scientific. Analytical grade Sodium Bromide ( $NaBr$ ), Sodium Nitrate ( $NaNO_3$ ), Sodium Thiosulphate ( $Na_2S_2O_3$ ) were obtained from Alfa Aesar.

#### 3.2 Sample Preparation

All samples were prepared in 20 ml vials. Concentration of methyl cellulose in the solution was adjusted to 5,15,25,35,45 g/L. Preparing methyl cellulose in cold water can be a difficult task as when the MC powder comes in contact with water, a gel layer is formed. This reduces the diffusion of water into the MC powder and results in the formation of macro-gelled particles with a very low rate of dissolution. Thus, literature has recommended to disperse the MC powder in hot water and then cooled under continuous stirring. This results in a homogenous solution.

1/3<sup>rd</sup> of the required volume of water was first heated to 80°C. Methyl cellulose powder was then added to the hot water with agitation. A magnetic stirring bar was used for mixing. The mixture was agitated until the particles were thoroughly wetted and evenly dispersed in water. For complete solubilization, the remainder of the water was then added as cold water. Once the dispersion reaches temperature at which methyl cellulose becomes water soluble, the powder dissolves and the viscosity increase. The solutions were then cooled at for 6-7 hours.

To investigate the effect salt on the transition temperature, 8 sodium salts were tested. The salts under investigation were  $Na_2PO_4$ ,  $NaCl$ ,  $Na_2SO_4$ ,  $NaF$ ,  $NaBr$ ,  $NaNO_3$ ,  $Na_2S_2O_3$ ,  $NaI$ .

Each of these salts in concentrations between 0 and 1M were added to the heated water before adding the MC powder. All samples were prepared using deionized water.

### 3.3 Sample Characterization

#### 3.3.1 Transition temperature measurement

Initial measurements for the transition temperature of the samples were made using a temperature-controlled water bath. Samples with varying concentrations MC and salt concentrations were stored in 20 ml vials and submerged in water bath. Starting from room temperature, the temperature of the water bath was increased in increments of  $5^{\circ}C$  and let to equilibrate for 10 minutes. The opacity of the sample was measured by placing a printed sheet of paper behind the vial. The temperature at which the printed words were no more visible was recorded as the transition temperature. The samples were tested again at temperatures around the previously recorded transition temperature. During this run the temperature was increased at increments of  $1^{\circ}C$ . This helped verify the previously recorded transition temperature.

#### 3.3.2 UV-VIS Spectroscopy

The UV-VIS spectra were tested using the Agilent Cary 6000i UV-VIS-NIR spectrophotometer with a wavelength range of 175-800 nm. The spectrophotometer was equipped with a heating and cooling stage using a Peltier temperature control system. A baseline correction was performed prior to running samples in the equipment. All samples were tested between the temperature range of  $20^{\circ}C - 70^{\circ}$ . The temperature was increased at the increments of  $10^{\circ}C$ . At temperatures close to the transition temperature recorded by previous tests, the temperature increments were made at  $5^{\circ}C$ . Rectangular, quartz cuvettes with a path length of 10 mm were used. The temperature at which 50% of the overall transmittance in the sol-gel transition was reached was defined as the transition temperature. The integral transmittance was calculated using the equation:

$$T_{int} = \int T(\lambda) E_{\lambda}(\lambda) d\lambda / \int E_{\lambda}(\lambda) d\lambda$$

Where  $T(\lambda)$  denoted spectral transmittance,  $E(\lambda)$  is the solar irradiance spectra in the wavelength between 200 – 800 nm for air mass 1.5 (corresponding to the sun standing 37° above the horizon

### 3.3.3 Freezing Resistance Test

Freeze resistance was tested by maintaining the samples at  $-10^{\circ}\text{C}$  for 90 minutes. MC samples of concentrations 15,25,35 g/L were examined. The effect of salt on the freeze resistance was investigated using a 25g/L MC solution with 0.6M NaF

### 3.3.4 Scanning Electron Microscopy in cryogenic mode (Cryo-SEM)

Cryo-SEM was performed on FEI NOVA nanoSEM Field Emission SEM. The cryo imaging utilizes the GATAN Alto 2500 cryo system. The cryo systems on the NOVA nanoSEM and the Quanta 3D FEG microscopes consist of a freezing unit, a turbo-pumped cryo preparation unit, and a cryo stage that attaches to the microscope stage. The cryo system permits flash freezing of samples in liquid nitrogen slush followed by high vacuum sublimation of unbound water, Pt coating to minimize charge build-up and imaging at temperatures down to  $\sim 160^{\circ}\text{C}$ . SEMs operate under some level of vacuum to minimize the scattering of electrons by gas molecules. This imposes certain requirements for sample preparation to ensure that the sample is compatible with the microscopy procedure. Furthermore, some provision must be made to dissipate the charge deposited at the sample from the electron beam by creating a conductive coating. Thus, cryo-SEM sample preparation consists of drying and coating procedures.

Prior to any observation, the hydrogel was frozen in slush nitrogen and then quickly introduced to the microscope chamber. Here the sample is held under vacuum in a low temperature state. The temperature of the sample was set at  $-140^{\circ}\text{C}$ . The peak of the sample is cut off/fractured using a knife. Cryo-fracturing exposes the internal structures of the sample for high resolution imaging. The sample is then sublimated for a few minutes at low temperature to remove the natural surface ice. Greater details of the sample can be revealed by carefully raising the temperature of the hydrated freeze fractured specimen to a temperature where the water in the sample begins to sublime. Sublimation can be stopped at any point by again lowering the



temperature. The sample was freeze dried at  $-80^{\circ}\text{C}$ . It is then sputter coated with platinum before it is transferred to the specimen chamber for SEM.

### **3.3.5 Dynamic Light Scattering**

Dynamic Light Scattering (DLS) measures time-dependent fluctuations in the scattered light, which are directly related to the rate of diffusion of the molecule through the solvent. This is used to measure the hydrodynamic radius of the particles in the solution. The equipment calculates the hydrodynamic radius from the analysis of the fluctuation of the intensity of the scattered light over time.

The DynaPro Plate Reader Dynamic was used to analyze the size of the particles in the MC aqueous polymer solution. An optical bottom microwell plate consisting of 384 wells was used for the measurements. The 2 samples under test were pipetted into separate wells, and the well plate was placed into the plate reader equipment. The equipment was used in a ‘fixed temperature scan’ setting. Each sample was tested at  $23^{\circ}\text{C}$  and  $70^{\circ}\text{C}$ . The default heating rate of the equipment was  $0.5^{\circ}\text{C}/\text{min}$ .

### **3.3.6 Window demonstration**

A window demonstration was performed in order to investigate the performance of the polymer under solar radiation. The window used for the demonstration had the dimensions of 6” x 6” x 7/16 “. The two glass substrates were separated by an aluminum spacer and sealed using a silicone sealant. The window glass had no tint or previously applied coating. A small portion of the silicone seal on one edge of the window was scrapped off. A 3mm hole was drilled through the aluminum spacer ensuring that no scrap from the drilling operation falls inside the window. A polymer solution consisting of 25 g/L MC along with 0.5M NaF was poured inside the window using a pipette. Once the window was filled with the polymer, it was sonicated for 10 minutes in a water bath to remove the air bubbles from the polymer. At the end, the opening was sealed using a tacky tape in order to prevent any polymer from spilling out.

## 4. RESULTS AND DISCUSSION

### 4.1 Transition temperature

MC solutions of concentrations between 5-55g/L were prepared and tested for their transition temperature. The viscosity of the sample increased as the concentration of MC was increased. The concentration of MC had to be limited to 55 g/L, as the solution became too viscous to continue mixing. It was observed that the transition of MC solution from clear to opaque state is not a drastic change but a gradual process. The opacity of the material changed homogeneously over the entire area without any streaking. Figure 12 shows the state of a 25g/L sample at increments of  $10^{\circ}\text{C}$ . The sample gains a white tinge at  $\sim 50^{\circ}\text{C}$ . Gradually the opacity of the material increases.

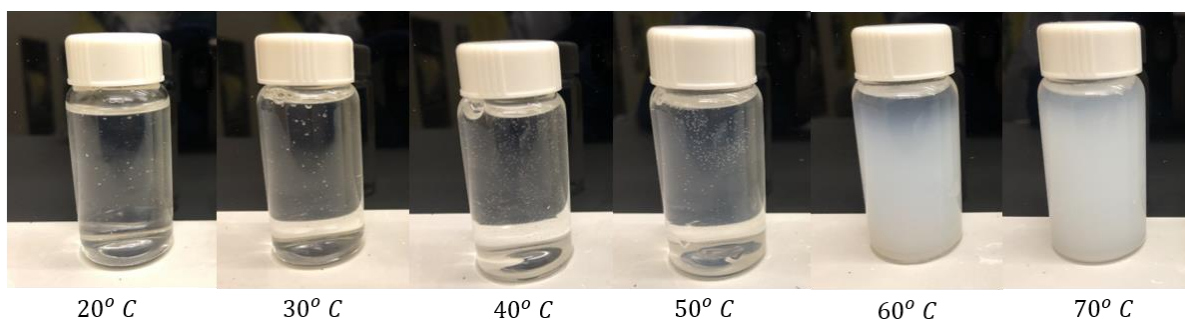


Figure 12 Optical states of a 25g/L MC sample at increasing temperatures

Figure 13 shows the transition temperatures for MC at concentrations between 5-55 g/L MC concentration. It can be seen that the transition temperature decreases as the concentration of MC increases. This is because at low MC concentration, the number of methyl groups present are less. Higher energy is required to initiate the intermolecular hydrophobic association. As the concentration of MC is increased, due to presence of larger number of methyl groups, lower amount of energy is required to initiate their hydrophobic association, resulting in a lower transition temperature. For further investigation, MC solutions between the concentrations 15-35g/L were used as the viscosity of solutions with MC concentrations higher than 35g/L was too high for our intended application, and the transition temperature of solutions with MC

concentration lower than 15g/L was higher than the transition temperature desired for our application.

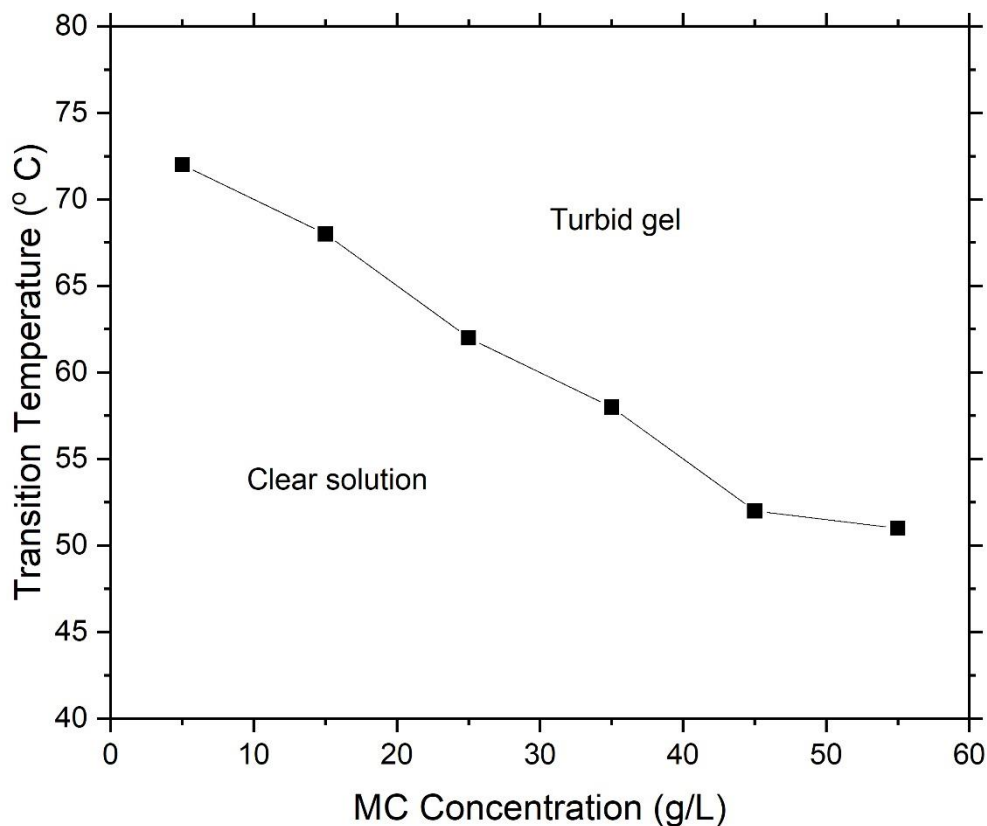


Figure 13 Transition temperature of MC as a function of MC concentration

## 4.2 UV-VIS Spectroscopy

Figure 14, a-c shows the change in transmittance in the MC aqueous solution sample at various MC concentrations and temperatures for wavelengths between 200-800 nm, measured using a UV-VIS spectrophotometer. It can be seen that for all concentrations under study, the transmittance through the sample at temperatures below the LCST is high. The 35 g/L sample displays a reduced transmittance at temperatures lower than its LCST as compared to 15, 25g/L concentration samples. This can be attributed to improper mixing and dissolution resulting from a high viscosity. At low temperature, MC fibers swell by taking in water, but increasing temperature drives out the water and shrinks the fibers, resulting in light scattering. As the temperature is

increased to the LCST, the transmittance through the sample reduces slightly. This corresponds to a milky white state of the sample, that is not completely opaque. For all the samples, this state is attained at temperatures close to  $60^{\circ}\text{C}$ . However, 15g/L MC sample shows a higher transmittance as compared to 25g/L MC sample which in turn shows a higher transmittance than the 35g/L MC sample. At a given temperature, higher concentration MC solution has a lower transmittance than a low concentration MC solution. This implies that the transition temperature or LCST is a function of the concentration of MC.

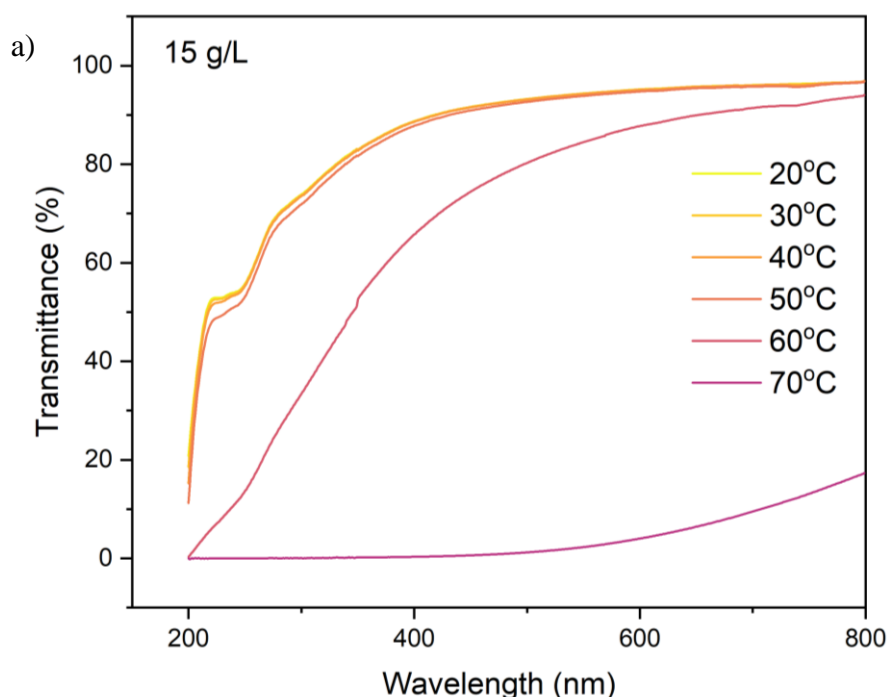
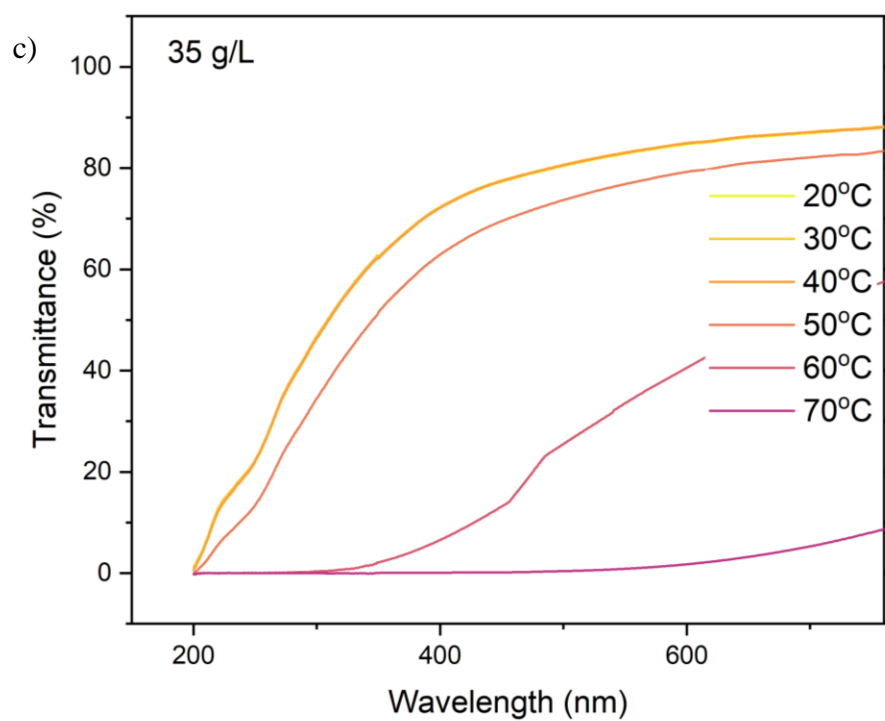
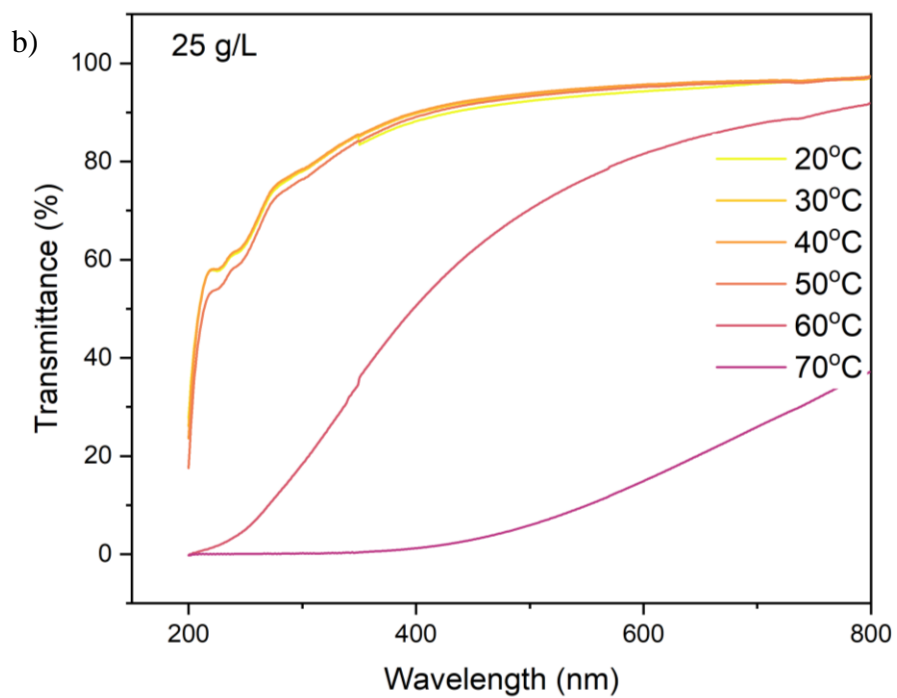


Figure 14 Transmittance of methyl cellulose at temperatures between  $20^{\circ}\text{C}$  –  $70^{\circ}\text{C}$  for a) 15g/L b) 25g/L c) 35 g/L methyl cellulose concentration

Figure 14 continued



The integral transmittance ( $T_{int}$ ) was measured based on the measured spectra in order to investigate the solar modulation ability of the sample. The following equation was used:

$$T_{int} = \int T(\lambda) E_{\lambda}(\lambda) d\lambda / \int E_{\lambda}(\lambda) d\lambda$$

Where,  $T(\lambda)$  is the measured transmittance spectra as a function of wavelength  $\lambda$ .  $E(\lambda)$  is the solar irradiance spectrum for air mass 1.5

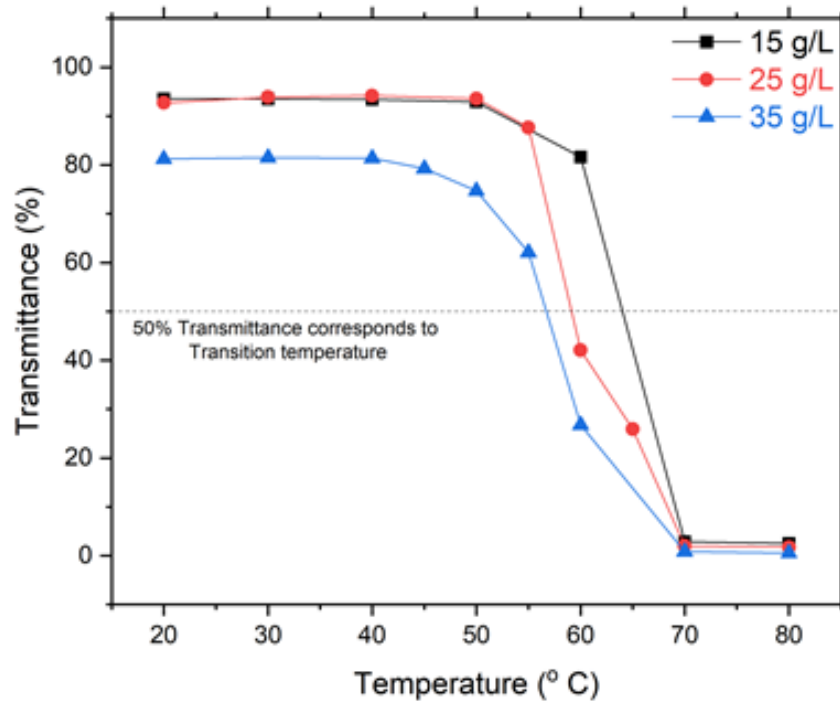


Figure 15 Transmittance of 15,25, 35g/L MC samples as a function of temperature

Figure 15 shows the transmittance of light for 15,25,35 g/L MC concentrations as a function of temperature. For each concentration, the transparent solution became progressively turbid above a critical temperature, which is defined at 50% transmittance value. To assist the reader in evaluating the terms in Figure 14, table 3 provides the transmittance values for 15, 25 and 35 g/L MC samples at temperatures between 20 – 80°C. It can be seen that the 15 and 25g/L

MC samples have a higher transmittance at room temperature as compared to the 35g/L sample. Low transmittance above the transition temperature for a 35 g/L aqueous MC solution can be attributed to improperly dispersed MC powder due to poor mixing and high viscosity of the sample. Change in the optical state of the sample from transparent to opaque occurs over a range of temperatures. Low temperatures show a transmittance value as high as 93.51%. At temperatures above the transition temperature, the transmittance attains a value close to 1%.

Table 3 Integral Transmittance % for 15,25, 35g/L MC samples as a function of temperature

MC Concentration \ Temperature (C)	15 (g/l)	25 (g/l)	35 (g/l)
20	93.51	92.70	81.23
30	93.48	93.88	81.47
40	93.39	94.19	81.37
50	92.93	93.56	74.73
60	81.61	42.05	26.73
70	2.87	2.00	0.83
80	1.50	1.76	0.54

The turbidity is caused by light scattering from the hydrophobic aggregates of MC. At low temperatures, water molecules form cage-like structures, also known as hydration layer<sup>60</sup>, around the hydrophobic methyl groups via hydrogen bonding. Above the transition temperature, the hydrophobic methyl groups lose their hydration layer and form hydrophobic associations with other methyl groups. The number of these hydrophobic associations increase with temperature, eventually leading to a three-dimensional polymer chain network. These results show that salts promote the release of water from MC fibers even at low temperatures.

### 4.3 Effect of Salts

Keeping the cation in the salt same while varying the anion allows us to study the effects of anions. Previous studies have concluded that the effect of anions is stronger than cations at water structuring because of the asymmetry of charge in a water molecule.<sup>78</sup> Sodium halide salts are chosen for this study. The concentration of MC was fixed at 25 g/L for this study. The salts studied were  $Na_2PO_4$ ,  $NaCl$ ,  $Na_2SO_4$ ,  $NaF$ ,  $NaBr$ ,  $NaNO_3$ ,  $Na_2S_2O_3$ ,  $NaI$ . From preliminary tests it was observed that there is a limit on the concentration of salt that can be mixed in the MC solution.

For example, concentration of  $Na_2S_2O_3$  had to be limited to 0.6M as a higher concentration would either lead to the sample being too viscous to be transported and give the sample a milky white color, or the solution precipitates, compromising its transparency. It was observed that the individual concentration limit of each salt was a function of the ionic charges. For example, the single charged ions showed a concentration limit of about 1 M, while the double-charged ion ( $SO_4^{2-}$ ) has a concentration limit of 0.1 M. The triple charged ion ( $PO_4^{3-}$ ) shows a concentration limit of 0.05 M. Thus, the concentration for  $NaI$  was varied between 0 and 0.8 M,  $Na_3PO_4$  between 0 and 0.05M,  $Na_2SO_4$  between 0 and 0.1M, and between 0 and 1M for rest of the salts while the MC concentration being fixed at 25g/L.

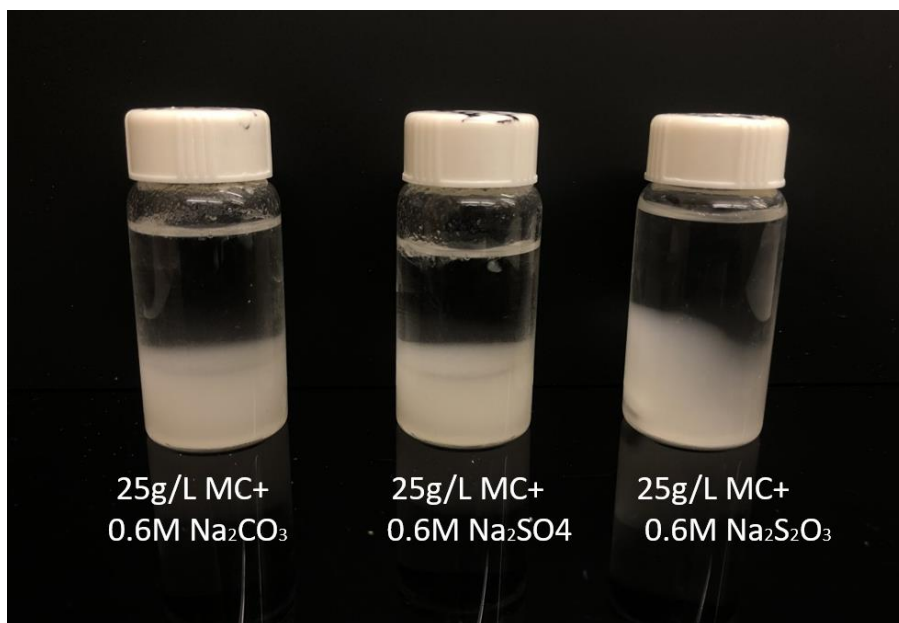


Figure 16 25g/L MC solution precipitation in presence of  $Na_2CO_3$ ,  $Na_2SO_4$ ,  $Na_2S_2O_3$

The transition temperatures for the salts under study at concentrations between 0 and 1M obtained are shown in Figure 17. It can be seen that the trends of all salts except  $NaI$  have a negative slope. It signifies that those salts cause salting-out, whereas  $NaI$  has a positive slope indicating salting-in behavior. The salting out strength of the salts can be understood by the magnitude of the slopes of salts. From Figure 16 it can be seen that  $Na_2PO_4$  has the highest magnitude of slope, indicating that a small increase in salt concentration leads to a drastic change in the transition temperature.



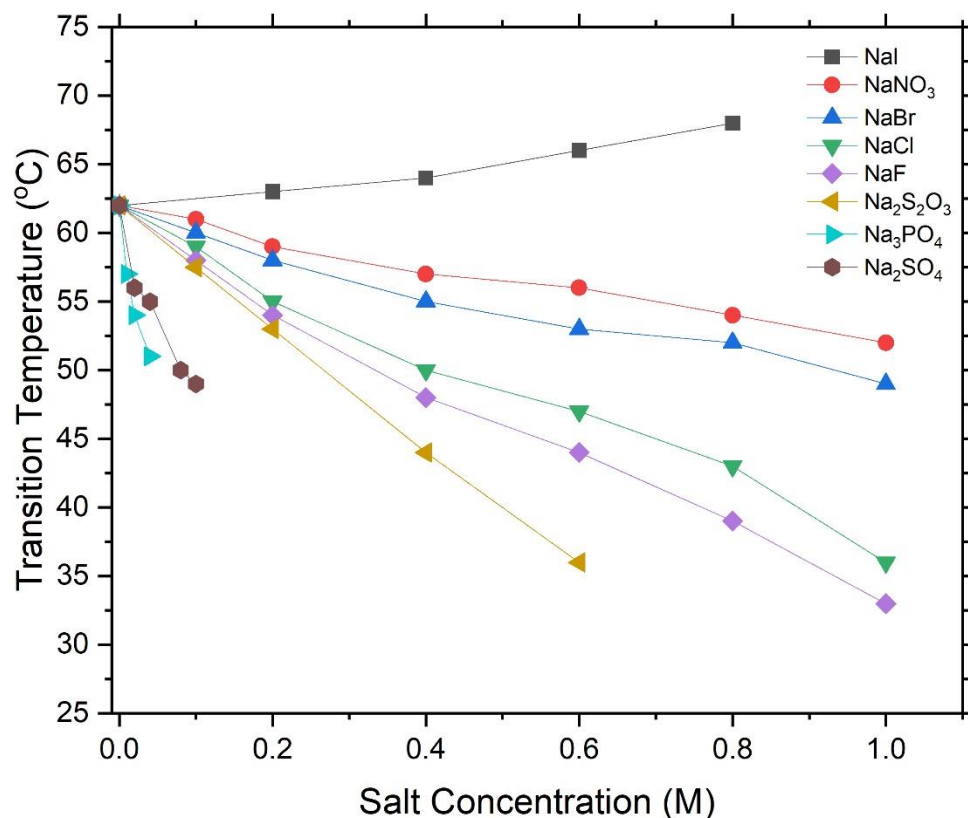


Figure 17 Change in transition temperature for a 25 g/L MC aqueous solution with the concentration of various sodium salts

When salts are added to MC solution, salts form hydrogen bonds with the water molecules that are stronger than the bond between water and MC chains. The four halide ions  $I^-$ ,  $Br^-$ ,  $Cl^-$ ,  $F^-$  and the nitrate ion  $NO_3^-$  carry a charge of -1. Another important consideration is the radii of the ions. The ionic radii of  $I^-$ ,  $Br^-$ ,  $Cl^-$ ,  $F^-$  are 2.16, 1.95, 1.81, 1.36 Å.<sup>79</sup> The effect of various salts can be studied by looking at their hydration energies. Hydration energy or hydration enthalpy is defined as the amount of energy released when one mole of ion undergoes hydration. It is a special case of dissolution energy with the solvent as water. Hydration energy is governed by the amount of attraction between ions and water molecules. It is affected by the ionic size and ionic charge. As charge on all the ions is the same, the ion with the smallest radii will

have the highest charge density and highest solvation strength. This explains why the ions with the same electronegativity affect the sol-gel transition of MC differently.

In case of anions with varying charges, both, the ionic size and charge need to be taken into consideration. As discussed earlier, it was observed during sample preparation that each salt had a limitation on the concentration that could be added to MC solution. Salts containing anions with a single charge showed a limit of 1M concentration in MC.  $Na_2S_2O_3$  showed a limit of 0.6 M,  $Na_2SO_4$  of 0.1M and  $Na_3PO_4$  of 0.05M. At concentrations above this limit, the MC solution was become too viscous for the magnetic stir bar to operate in the solution.  $PO_4^{3-}$  ion carries a charge of -3,  $SO_4^{2-}$ ,  $S_2O_3^{2-}$  ions carry a charge of -2. It can be concluded that higher the charge on the ion, stronger is the salting-out strength. Thus, the ability of salts to tune the transition temperature depends on the charge density which impacts the salting-out strength of the ion. Ions possessing a higher charge have the ability to form strong bonds with water molecules. Ions with a larger ionic radii may have a low charge density resulting in less water being attracted to the ions.

Table 4 Radii and free energies of hydration for selected ions <sup>80</sup>

Ion	Radius	Hydration energy ( $\Delta G_{hydr}/$ $KJ\ mol^{-1}$ )
$F^-$	1.33	-465
$I^-$	2.16	-275
$NO_3^-$	1.79	-300
$CO_3^{2-}$	1.78	-1315
$SO_4^{2-}$	2.30	-1080
$PO_4^{3-}$	2.38	-2725

$NaI$  is the only salt under study that shows a transition temperature vs concentration trend line that has a positive slope. The transition temperature of the solution increases when salting-in salts are added to a solution.  $I^-$  is a big, singly charged ion that acts like a hydrophobic molecule.<sup>69</sup>  $I^-$  ion's interaction with water is weaker than water itself.<sup>69</sup> Such big ions disperse the MC chains in the solution such that the chances of linking of MC chains reduce. In this case more energy is

required for the MC chains to form hydrophobic associations, as compared to a pure MC solution. Thus, gelation occurs at a higher temperature. Delayed gelation process is referred to as salt suppressed sol-gel transition.<sup>69</sup>

#### 4.4 Freeze Resistance

Table 5 shows 15,25,35 g/L MC solutions maintained at  $-5^{\circ}C$  and  $-10^{\circ}C$  for 90 minutes. It can be seen that the transparency of all three samples reduced drastically at  $-5^{\circ}C$ . The samples maintained the reduced transparency states at  $-10^{\circ}C$ . To understand the effect of salt on freeze resistance, 25g/L MC samples with 0.4 and 0.6 M *NaF* were tested. It was observed that neither sample with salt show any change in transparency at  $-5^{\circ}C$ . The sample with 0.4M *NaF*, however, froze at  $-10^{\circ}C$ . The sample with 0.6M *NaF* did freeze up till  $-10^{\circ}C$ .

Table 5 Freeze resistance of pure MC aqueous solutions of varying MC concentrations.

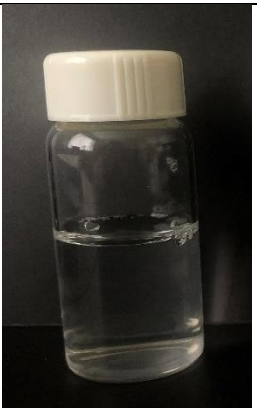




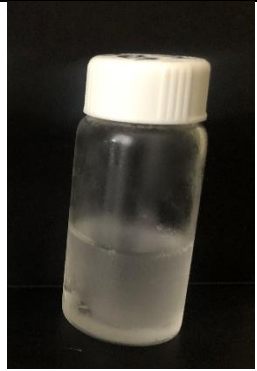



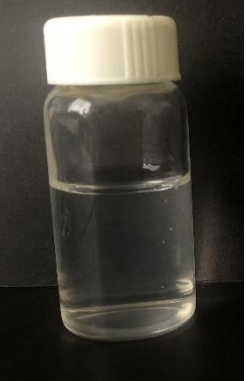

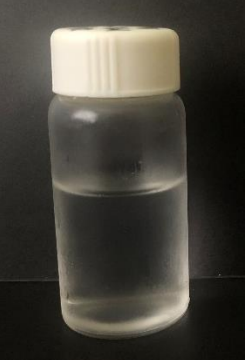



MC Concentration Temperature	15 g/L	25 g/L	35 g/L
23°C			
-5°C			
-10°C			

Table 6 Freeze resistance of MC aqueous solutions with 0.4 M and 0.6 M NaF

<div>MC and salt Concentration</div> <div>Temperature</div>	25g/L + 0.4 M NaF	25g/L MC+ 0.6 NaF
23°C		
-5°C		
-10°C		

The reduced transparency of MC samples at lower temperatures is a result of freezing of water. It was seen that all the samples froze, irrespective of the MC concentration. However, MC samples with added salts did not freeze as the salt depressed the freezing point of water. Freezing point of pure water can be depressed by the addition of a solvent such as salt. Salts form a strong hydrogen bonding with water which prevents water from freezing. The temperature at which water freezes depends on the concentration of salts. Thus, increasing the salt concentration improves the freeze resistance of the MC sample.

#### **4.5 Size distribution**

Dynamic Light scattering is a measurement technique for characterising the particle size in suspension and emulsions. It is based on the brownian motion of the particles. The light scattered by the particles contains information about the diffusion speed and thus on the size distribution. The effect of size distribution of MC was characterized using a DLS. This test was used to investigate the particle size distribution of the prepared MC sample at temperatures below and above the transition temperature. Figures 18 & 19, a), b) show the size distribution of the particles in the MC solution at temperatures above and below the transition temperature for 10 g/L and 15 g/L MC concentration.

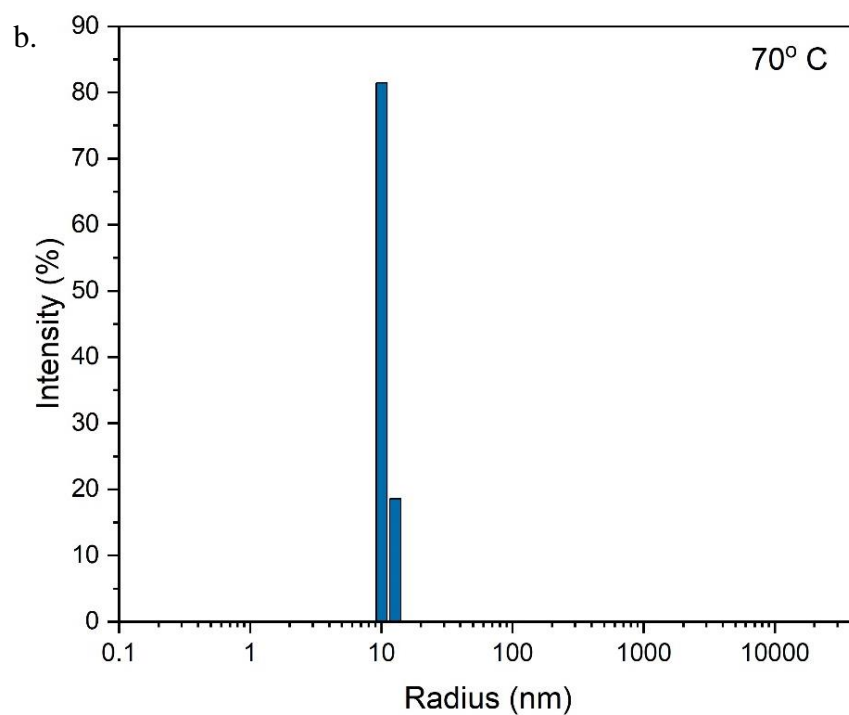
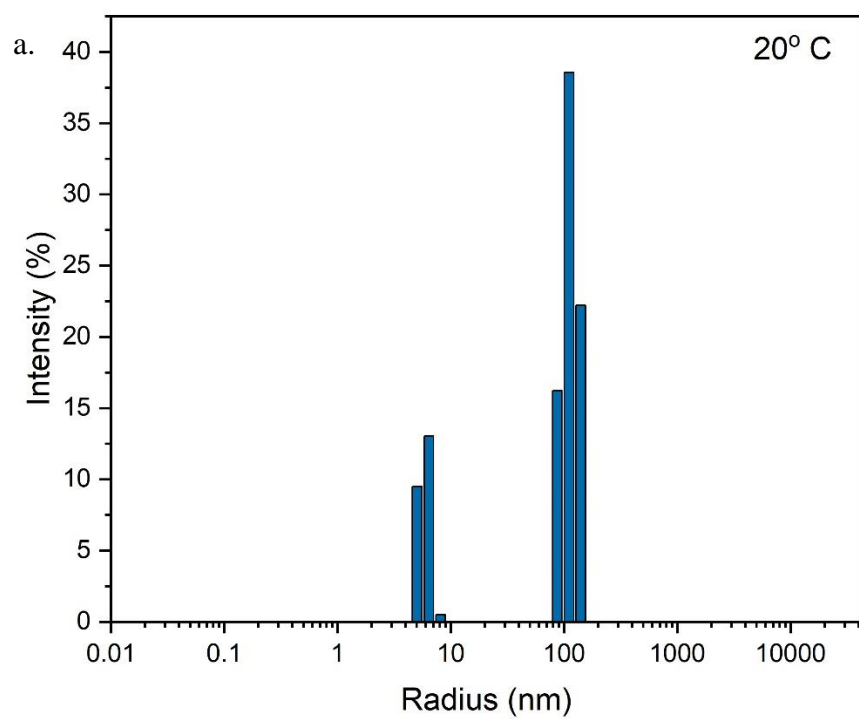


Figure 18 Particle size distribution of 10 g/L MC sample at a) 20°C and b) 70°C using DLS

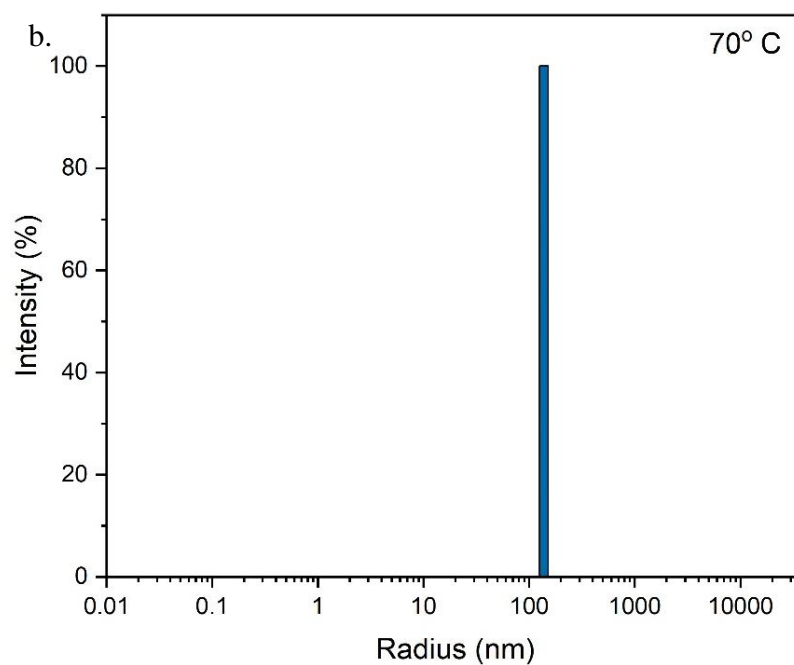
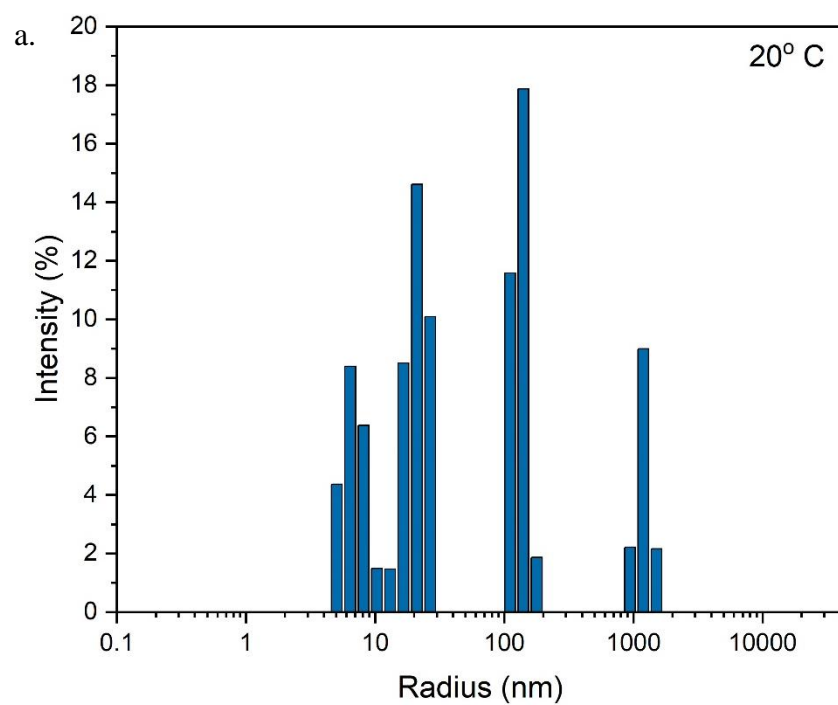


Figure 19 Particle size distribution of 15 g/L MC sample at a) 20°C and b) 70°C using DLS



Figure 17 shows the particle size distribution in a 10g/L MC sample. At temperature below the transition temperature ( $20^{\circ}\text{C}$ ), the highest scattering intensity is due particles of size of 100 nm. As the temperature of the sample is raised above, the transition temperature (*i. e.*  $70^{\circ}\text{C}$ ), the size of the scattering centers/particles is 10 nm which leads to a scattering intensity of 81%. Similar observations were made for the 15 g/L MC sample. At  $20^{\circ}\text{C}$ , the size distribution was broader as compared to the 10g/L MC sample. As the temperature was increased to  $70^{\circ}\text{C}$ , the average particle size recorded was 150nm which resulted in a 99% scattering intensity. As it can be observed, the particle size reduced as the temperature increased above the transition temperature. This is probably caused by the swelling and deswelling behavior of MC hydrogel. At low temperature, MC fibers swell by taking in water, but increasing temperature drives out the water and shrinks the fibers, resulting in light scattering.

As discussed in section 2.4, the light scattering in the opaque state is due to the formation of polymer globules that act as the scattering centers for light. Thus, it is expected that the size of the scattering centers should be greater at  $70^{\circ}\text{C}$  than that at  $20^{\circ}\text{C}$ . However, this is not observed. This can be caused to way a DLS equipment functions. A DLS consists of a monochromic light source, usually a laser, that is passed through the sample. When the light hits small particles, the light is scattered in all directions as long as the particles are small compared to the wavelength of the incident light. As the particles in the suspension undergo Brownian motion, the scattering intensity fluctuates over time. The detector records the fluctuations in the intensity of the scattered light over time. The application of DLS is often limited due to a phenomenon called as ‘multiple scattering’. For DLS particle sizing, the sample needs to be water clear or very slightly hazy. In case the sample is too concentrated, the measured particle size will be inaccurate due to multiple scattering effect. Multiple scattering occurs when the particle concentration is too high where the light gets scattered from a single particle and is re-scattered by others in the suspension. This can result in a very weak signal reaching the detector in the DLS. This causes the measured particle size to be artificially low. Thus, if the solution is white, it should be diluted further before attempting the DLS measurements. In order to get accurate measurements of the size of the scattering centers in MC, the solution under test should either be a very dilute solution, or the temperature of the solution should be kept slightly below the LCST, so that the solution is hazy and not completely opaque.

#### 4.6 Scanning Electron Microscopy

In order to obtain information about the water-matrix arrangement in the MC hydrogel, cryo-SEM was performed. The sample is rapidly frozen in slush nitrogen to preserve the structure of the sample. The obtained SEM micrographs obtained for 10g/L MC concentration sample are shown in figure 20.

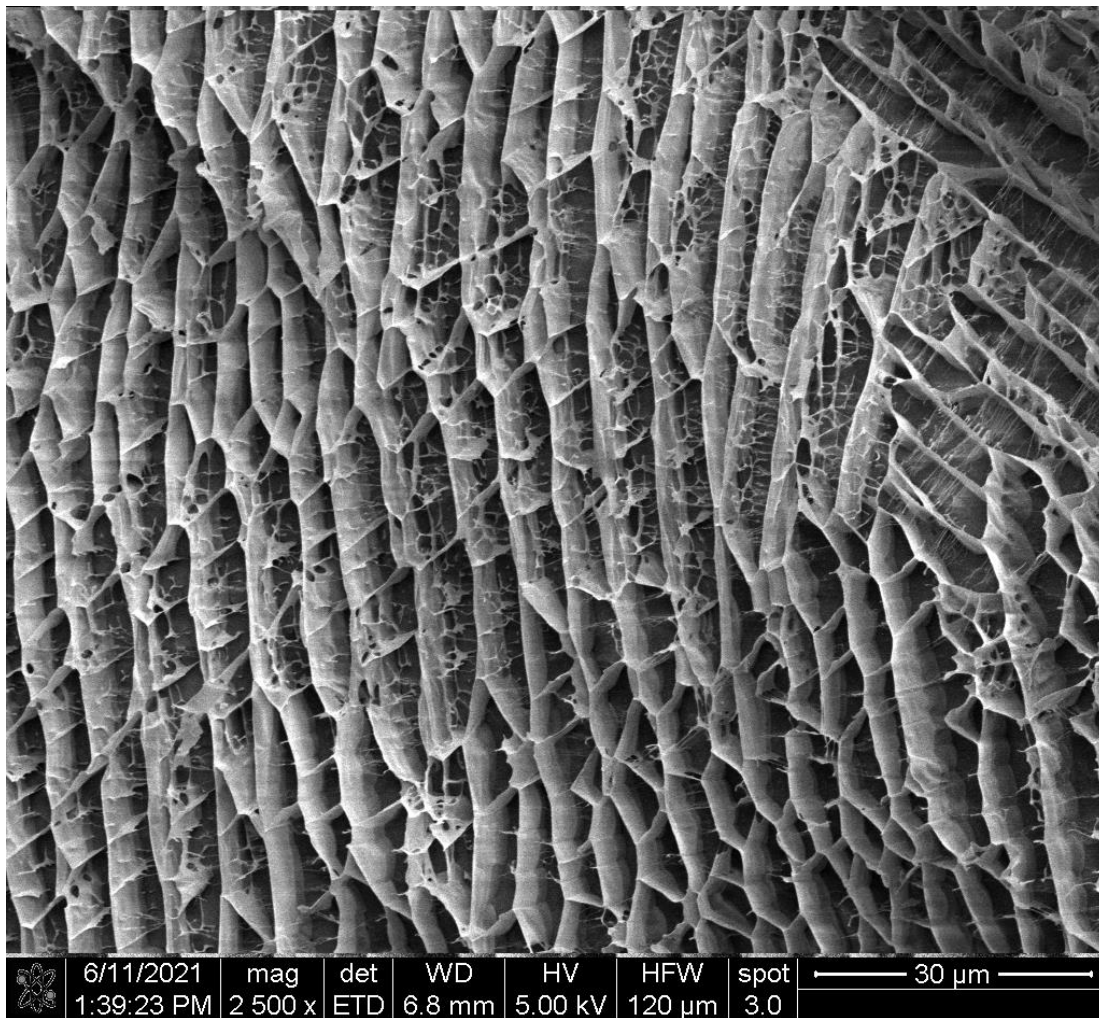
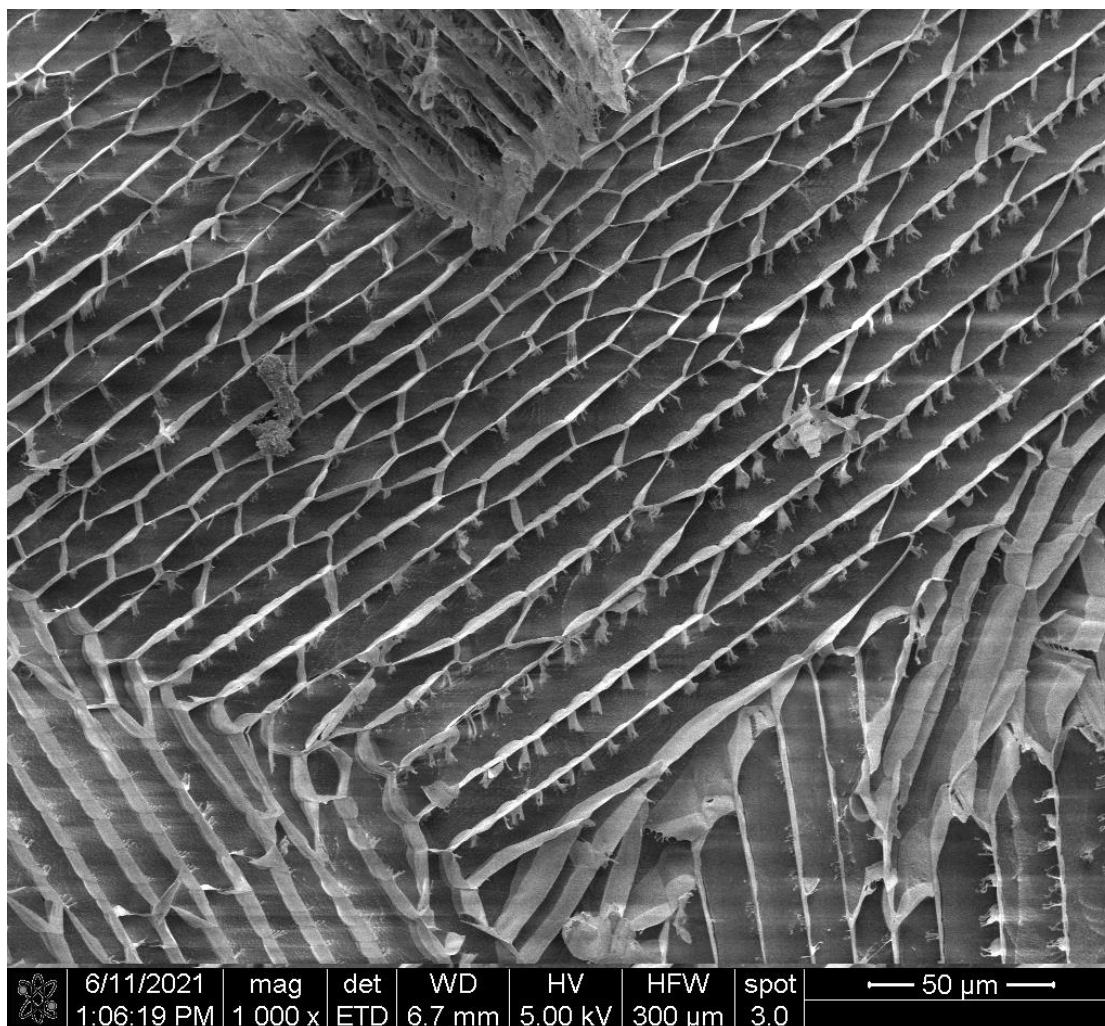


Figure 20 Cryo-SEM micrographs of the porous network formed within the 25 g/L MC hydrogels.

Figure 20 continued



It can be seen from the SEM micrographs in figure 20 that the use of slushy nitrogen for the preparation of sample disrupts the native structure of MC network. Sample preparation procedures for cryo-SEM can lead to some interference in SEM imaging and analysis. The changes occurring in the sample during cryo-sample preparation is shown in the schematic in figure 21. When samples are cryo-fixed using the nitrogen slush, ice crystals start to form in the sample. As the ice crystals grow in size, they exclude the polymer chains into the area of unfrozen water. This causes the polymer chains to be sequestered between the boundaries of neighboring ice crystals. This ultimately leads to the formation of honeycomb-like structure. This can be seen in the schematic shown in figure 20. A) Shows the native state of the polymer solution B) shows the formation of ice crystals resulting in the polymer chains being sequestered into the unfrozen parts of water C) a honeycomb structure formed by dense polymer walls as a result of ice crystal formation.<sup>81,82</sup>

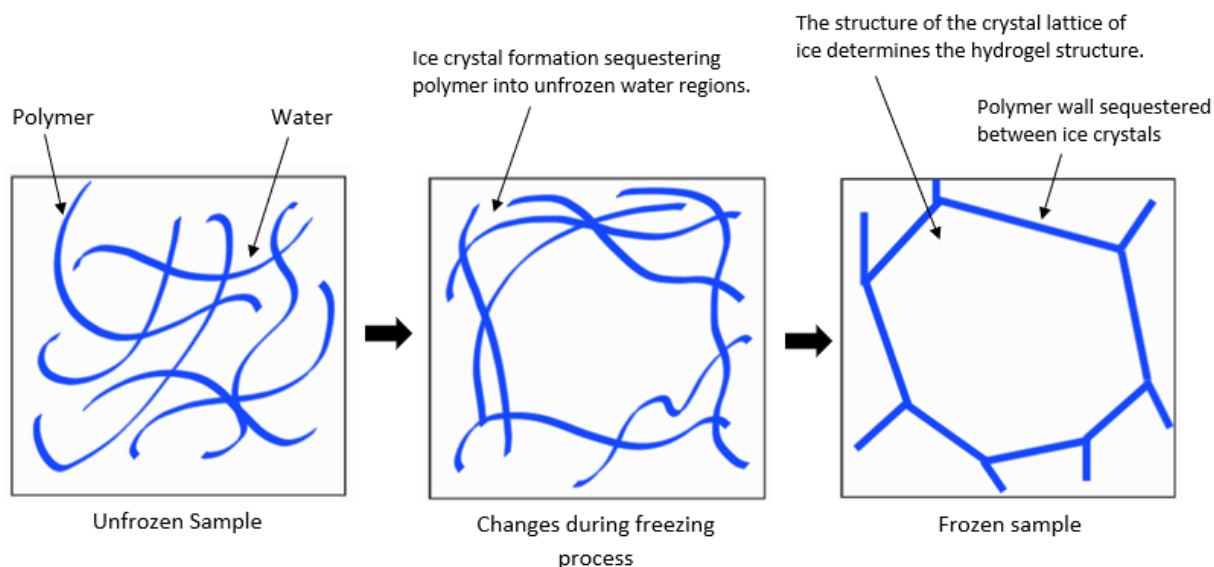


Figure 21 Mechanism for the freezing process of the sample when using slushy nitrogen for sample preparation for cryo-SEM

Freeze drying, also known as lyophilization can be used as an alternative to cryo-SEM as sample preparation method. Freeze drying is widely used for sample preparation of hydrogels as this process has unique sample structure preservation properties. It is a process in which a completely frozen sample is placed under vacuum in order to remove water or other solvents from

the sample. The ice is allowed to change directly from a solid state to a vapor phase, without passing through a liquid phase. Further, SEM can be used to study its surface morphology,

#### 4.7 Window demonstration

For testing the compatibility of the polymer, a model window was filled with the thermo-responsive polymer and exposed to sunlight. The window used for the demonstration had the dimensions of 6" x 6" x 7/16 ". The two glass substrates were separated by an aluminum spacer. The window glass had no tint or previously applied coating. A hole was drilled through the spacer to make provision for the polymer to be poured inside. Once the polymer was poured, the opening was sealed using a butyl tape. Figure 22 a is the picture of the window taken early in the morning and Fig 22 b is the picture of the window captured in the afternoon.



Figure 22 Model thermochromic window demonstration a) without sunlight exposure b) after exposure to solar radiation

The polymer was filled to the brim of the window. Air bubbles present in the polymer were removed by sonication. When the window was exposed to sunlight, the transition of the polymer began when the temperature of the glass reached the transition temperature. As the polymer has a broad switching temperature, the window exhibited a uniformly tinted appearance as the temperature increased and reached the transition temperature. It was observed that there was no polymer overflowing after the sol-gel transition. This indicates that the sol-gel transition does not result in a volume change in polymer. The transition of the polymer from clear to opaque state was slow as the transition started after the temperature of the glass reached the transition temperature of the polymer.

## 5. CONCLUSION

This chapter summarizes the major conclusions in the research and provides some ideas for future work.

### 5.1 Conclusions

Current smart window commercialization effort is based on the use of conventional electrochromic windows. However, electrochromic suffer from disadvantages such as high manufacturing and maintenance cost, complicated installation and maintenance etc. Thermochromics are potential candidates to replace the conventional electrochromic as they have a low manufacturing and maintenance cost and can be offered as a retrofit system.

The work we have introduced in this thesis contributes to the effort of developing a thermochromic window system. In this work we have introduced a cellulose based smart thermochromic window system. The proposed technology autonomously modulated the transmittance of solar radiation in response to the ambient temperature. The system utilizes a sustainable, earth abundant and cost effective thermo-responsive material to transform existing windows to a thermally dynamic smart window system. The material is such that it can transits between low and high optical states at a designated threshold temperature known as the LCST or transition temperature.

Thermo-responsive Methyl Cellulose hydrogel was investigated as a potential alternative material for thermochromic window systems. The ability of MC to transit from a transparent to opaque state was demonstrated. It was observed that the transition between optical states occurs over a range of temperatures. UV-VIS spectroscopy was used to precisely record the transmittance through the samples at varying temperatures. Spectroscopic measurements showed that the transparent MC solution becomes progressively opaque over a range of temperatures. For a cuvette of 10 mm pathlength, it was assumed that the temperature corresponding to 50% transmittance is the transition temperature for that sample. Such measurements were made for aqueous MC solutions with increasing MC concentrations. It was concluded that the transition temperature is a function of the MC concentration. The sol-gel transition of MC occurs at a lower temperature when the concentration of MC is increased. The sol-gel transition mechanism of MC is related to the



microscopic phase separation. At temperatures below the transition temperature, the MC chains are hydrated by water molecules. Increasing temperature above the transition temperature results in the breaking of hydrogen bonds between the water molecules and the cellulose chains. This enables the hydrophobic groups to move closer to form aggregates which serve as the scattering centers for light.

It is possible to tune the transition temperature of the MC aqueous solution either by adjusting the DOS of MC, concentration of MC or by using additives such as salts. This thesis systematically studied the effect of addition of various salts on the transition temperature of MC. It was found that the effect of salt on the transition temperature of MC is dictated by the type of salt and its concentration. The effect of different anions was investigated and reported in this thesis. Our results were found to be in close agreement with the sequence of the Hofmeister series. It was observed that the transition temperature could either be increased or decreased for a constant MC concentration by varying the type of salt. The chaotropic salt under study in this work, *NaI*, resulted in an increase in the transition temperature. Kosmotropic salts under study, *Na<sub>3</sub>PO<sub>4</sub>*, *NaCl*, *Na<sub>2</sub>SO<sub>4</sub>*, *NaF*, *NaBr*, *NaNO<sub>3</sub>*, *Na<sub>2</sub>S<sub>2</sub>O<sub>3</sub>*, resulted in a decrease in the transition temperature for a constant MC concentration. It was observed that the salting out strength of each salt was different. It was concluded that the ability of different salts to cause salting out depended on various factors such as the ionic radii, the electronegativity and the hydration energy. Sodium phosphate was observed to have the highest salting out strength whereas sodium nitrate has the lowest salting out strength. Various permutations between the MC concentration, type of salt and salt concentration can allow the design of a thermo-responsive material for a thermochromic window for application in a certain geographic location.

The freeze resistance of pure MC was tested and compared to the freeze resistance of a MC solution with traces of salt. It was observed that pure MC samples showed poor freeze resistance irrespective of the concentration of MC. However, the freeze resistance improved drastically on the addition of salt. The improved freeze resistance in presence of salts is due to the strong hydrogen bonding between water and salt ions.

Thus, this research proposed a new thermochromic window technology that can not only be implemented in new window installation but also can be offered as a retrofit system. This study can be a useful tool to promote awareness and interest in thermochromic window systems.



## 5.2 Future Works

This study developed a cellulose based thermochromic smart window retrofit system. There are several aspects where the current work can be improved, and further research can be conducted for broadening and scope and capabilities of thermochromic smart windows.

Current experiments were limited to the performance of the window in the visible part of the electromagnetic spectrum. It is important to investigate the performance of the thermochromic material in the IR range, in order to calculate the heat shielding capacity of windows. Such measurements can be used to calculate the Solar Heat Gain Coefficient (SHGC) of the thermochromic window. The SHGC indicates the fraction of incident solar radiation admitted through a window and released indoor.

Most of the double pane windows consists of a layer of argon or air sandwiched between the two layers of glass. The type of gas affects the energy efficiency of the window as the thermal conductivity of the gas differs. Argon has a lower thermal conductivity as compared to air. Thus, argon filled window have better insulating properties as compared to air filled windows. Replacing the layer of insulating gas with a polymer can negatively affect the performance of windows by increasing the conductive heat gain. Measurement of thermal conductivity of the polymer is important in this regard. Use of a triple pane window with argon filled in one space and the polymer filled in the other could be an option worth examining further. The use of argon can limit the heat gain via conduction and polymer can limit the solar heat gain via transmission.

In interest of achieving energy reduction, it is important to analyze the performance of the window. Detailed energy modeling can be used estimate the overall impact on building heat load, lighting gains and energy use compared to standard and dynamic windows. Building energy modelling programs such as EnergyPlus (US DOE), eQUEST and numerous other commercial products enable the designer to develop models to predict the energy performance of the building. The input data file (ODF) describes the geometry of the simulated building, construction material, glazing characteristics, internal loads, mechanical equipments, HVAC operations and human occupancy schedules. Such simulations can be used to calculate certain energy performance characteristics. The U-factor is the rate at which the window conducts non-solar heat flow. The Solar Heat Gain Coefficient (SHGC) is the fraction of solar radiation admitted through a window- either transmitted directly and/or absorbed, and subsequently released as heat indoor. Lower SHGC value of the window indicates less solar heat transmission and great shading ability.

To validate the performance of the system, tests were performed on smaller samples in this work. However, a full-scale demonstration of the proposed technology in a test room can be helpful in understanding the performance of the window and gauging its suitability as a retrofit option. Testing the window in a controlled environment can help study its cost saving performance in varying temperature conditions by replicating the 8 climate zones (hot-humid, hot-dry, mixed-dry, mixed-humid, marine, cold, very cold, and subarctic) defined by ASHRAE. The durability and longevity of the product can be tested.

Although single hydrogel smart windows show capability of modulating transmittance of sunlight, multifunctional requirements from the window can be addressed by designing composite hydrogel systems. Composite hydrogel systems can help achieve desired multifunctionalities like faster switching speeds, lower transition temperatures, regulation of solar spectrum waveband separately, etc. Hydrogel based thermochromic windows effectively regulate the transmission of visible light. Whereas,  $VO_2$  based smart windows regulate the IR light transmission more effectively.<sup>3</sup> Thus, designing composite hydrogel systems for thermochromic windows can offer the advantage of flexible tuning of daylight and solar gain admission.

## REFERENCES

1. Pérez-Lombard, L., Ortiz, J. & Pout, C. A review on buildings energy consumption information. *Energy Build.* **40**, 394–398 (2008).
2. Isaac, M. & van Vuuren, D. P. Modeling global residential sector energy demand for heating and air conditioning in the context of climate change. *Energy Policy* **37**, 507–521 (2009).
3. Ke, Y. *et al.* Emerging Thermal-Responsive Materials and Integrated Techniques Targeting the Energy-Efficient Smart Window Application. *Adv. Funct. Mater.* **28**, 1–18 (2018).
4. U.S. energy consumption fell by a record 7% in 2020 - Today in Energy - U.S. Energy Information Administration (EIA). <https://www.eia.gov/todayinenergy/detail.php?id=47397>.
5. Use of energy in homes - U.S. Energy Information Administration (EIA). <https://www.eia.gov/energyexplained/use-of-energy/homes.php>.
6. Shishegar, N. & Boubekri, M. Natural Light and Productivity: Analyzing the Impacts of Daylighting on Students' and Workers' Health and Alertness. *Int. J. Adv. Chem. Eng. Biol. Sci.* **3**, 1–6 (2016).
7. Quadrennial Technology Review. Increasing Efficiency of Building Systems and Technologies. *An Assess. Energy Technol. Res. Oppor.* 143–181 (2015).
8. *Energy Efficiency Trends in Residential and Commercial Buildings.* (2008).
9. Wang, Y., Runnerstrom, E. L. & Milliron, D. J. Switchable Materials for Smart Windows. *Annu. Rev. Chem. Biomol. Eng.* **7**, 283–304 (2016).
10. Schneider, J. & Seeboth, A. Natural Thermotropic Materials For Solar Switching Glazing. *Materwiss. Werksttech.* **32**, 231–237 (2001).
11. Seeboth, A., Schneider, J. & Patzak, A. Materials for intelligent sun protecting glazing. *Solar Energy Materials and Solar Cells* vol. 60 263–277 (2000).
12. Resch, K. & Wallner, G. M. Thermotropic layers for flat-plate collectors-A review of various concepts for overheating protection with polymeric materials. *Solar Energy Materials and Solar Cells* vol. 93 119–128 (2009).
13. Watanabe, H. Intelligent window using a hydrogel layer for energy efficiency. *Sol. Energy Mater. Sol. Cells* **54**, 203–211 (1998).
14. Smart Glass Market by Technology, Application, Geography | COVID-19 Impact Analysis | MarketsandMarkets™. <https://www.marketsandmarkets.com/Market-Reports/smart-glass-market-907.html>.

15. Global Smart Glass Market Size & Share Report, 2021-2028. <https://www.grandviewresearch.com/industry-analysis/smart-glass-market>.
16. View Dynamic Glass. Energy benefits of View Dynamic Glass in workplaces. 1–10 (2017).
17. SONTE - Smart film for your windows and panes. <http://sonte.com/>.
18. RavenWindow | Smart Glass Windows | Smart Windows From RavenWindow. <https://www.ravenwindow.com/>.
19. licrivision® | Merck KGaA, Darmstadt, Germany. <https://www.emdgroup.com/en/brands/pm/licrivision.html>.
20. Products | Saint-Gobain. <https://www.privalite.com/en/products>.
21. Sala, R. L., Gonçalves, R. H., Camargo, E. R. & Leite, E. R. Thermosensitive poly(N-vinylcaprolactam) as a transmission light regulator in smart windows. *Sol. Energy Mater. Sol. Cells* **186**, 266–272 (2018).
22. Electrochromic windows an overview.pdf.
23. The Pros and Cons Of Smart Glass (Smart Windows) – The Home Hacks DIY. [https://www.thehomehacksdiy.com/the-pros-and-cons-of-smart-glass/#1\\_High\\_Price\\_around\\_100m<sup>2</sup>](https://www.thehomehacksdiy.com/the-pros-and-cons-of-smart-glass/#1_High_Price_around_100m2).
24. Oh, S. W., Kim, S. H. & Yoon, T. H. Control of Transmittance by Thermally Induced Phase Transition in Guest–Host Liquid Crystals. *Adv. Sustain. Syst.* **2**, 1–5 (2018).
25. Doane, J. W., Golemme, A., West, J. L., Whitehead, J. B. & Wu, B.-G. Polymer Dispersed Liquid Crystals for Display Application. *Mol. Cryst. Liq. Cryst. Inc. Nonlinear Opt.* **165**, 511–532 (1988).
26. Casini, M. Active dynamic windows for buildings : A review. *Renew. Energy* **119**, 923–934 (2018).
27. The IUPAC Compendium of Chemical Terminology. in (International Union of Pure and Applied Chemistry (IUPAC)).
28. Ke, Y. *et al.* Smart Windows: Electro-, Thermo-, Mechano-, Photochromics, and Beyond. *Adv. Energy Mater.* **9**, 1–38 (2019).
29. Li, S. Y., Niklasson, G. A. & Granqvist, C. G. Thermochromic fenestration with VO<sub>2</sub>-based materials: Three challenges and how they can be met. *Thin Solid Films* **520**, 3823–3828 (2012).
30. Zrínyi, M. *et al.* Smart gel-glass based on the responsive properties of polymer gels. *Polym. Adv. Technol.* **12**, 501–505 (2001).

31. Warwick, M. E. A. & Binions, R. Advances in thermochromic vanadium dioxide films. *J. Mater. Chem. A* **2**, 3275–3292 (2014).
32. Zhou, Y., Cai, Y., Hu, X. & Long, Y. Temperature-responsive hydrogel with ultra-large solar modulation and high luminous transmission for ‘smart window’ applications. *J. Mater. Chem. A* **2**, 13550–13555 (2014).
33. Wang, S. *et al.* Warm/cool-tone switchable thermochromic material for smart windows by orthogonally integrating properties of pillar[6]arene and ferrocene. *Nat. Commun.* 1–9 doi:10.1038/s41467-018-03827-3.
34. Tang, Y. *et al.* Programmable Kiri-Kirigami Metamaterials. *Adv. Mater.* **29**, 1–9 (2017).
35. Klouda, L. & Mikos, A. G. Thermoresponsive hydrogels in biomedical applications. *European Journal of Pharmaceutics and Biopharmaceutics* (2008) doi:10.1016/j.ejpb.2007.02.025.
36. Zhou, Y. *et al.* Hydrogel smart windows. *J. Mater. Chem. A* **8**, 10007–10025 (2020).
37. Deshmukh, S., Mooney, D. A., McDermott, T., Kulkarni, S. & Don MacElroy, J. M. Molecular modeling of thermo-responsive hydrogels: Observation of lower critical solution temperature. *Soft Matter* **5**, 1514–1521 (2009).
38. La, T. G. *et al.* Highly Flexible, Multipixelated Thermosensitive Smart Windows Made of Tough Hydrogels. *ACS Appl. Mater. Interfaces* **9**, 33100–33106 (2017).
39. Wang, M. *et al.* Binary solvent colloids of thermosensitive poly(N -isopropylacrylamide) microgel for smart windows. *Ind. Eng. Chem. Res.* **53**, 18462–18472 (2014).
40. Jain, S., Sandhu, P. S., Malvi, R. & Gupta, B. Cellulose derivatives as thermoresponsive polymer: An overview. *J. Appl. Pharm. Sci.* **3**, 139–144 (2013).
41. Nakamura, C. *et al.* Thermoresponsive, Freezing-Resistant Smart Windows with Adjustable Transition Temperature Made from Hydroxypropyl Cellulose and Glycerol. *Ind. Eng. Chem. Res.* **58**, 6424–6428 (2019).
42. Ding, Y. *et al.* Multiple Stimuli-Responsive Cellulose Hydrogels with Tunable LCST and UCST as Smart Windows. *ACS Appl. Polym. Mater.* **2**, 3259–3266 (2020).
43. Bwatanglang, B., Musa, Y. & Yusof, N. A. Market analysis and commercially available cellulose and hydrogel-based composites for sustainability , clean environment , and human health. (2020) doi:10.1016/B978-0-12-816789-2.00003-1.
44. Tian, Y., Ju, B., Zhang, S., Duan, X. & Dong, D. Preparation and phase transition behaviors of temperature-responsive 3-butoxy-2-hydroxypropyl hydroxyethyl celluloses. *J. Biomater. Sci. Polym. Ed.* **26**, 1100–1111 (2015).

45. Chang, C. & Zhang, L. Cellulose-based hydrogels : Present status and application prospects. *Carbohydr. Polym.* **84**, 40–53 (2011).
46. Khan, F., Tare, R. S., Oreffo, R. O. C. & Bradley, M. Versatile Biocompatible Polymer Hydrogels : Scaffolds for Cell Growth \*\*. 978–982 (2009) doi:10.1002/anie.200804096.
47. Thirumala, S., Gimble, J. & Devireddy, R. Methylcellulose Based Thermally Reversible Hydrogel System for Tissue Engineering Applications. *Cells* **2**, 460–475 (2013).
48. Zhang, Z. *Switchable and Responsive Surfaces and Materials for Biomedical Applications*. *Switchable and Responsive Surfaces and Materials for Biomedical Applications* (2015). doi:10.1016/C2013-0-16356-8.
49. Wu, D. *et al.* Fabrication of Supramolecular Hydrogels for Drug Delivery and Stem Cell Encapsulation. 10306–10312 (2008).
50. Katsoulos, C., Karageorgiadis, L., Vasileiou, N. & Asimellis, G. Customized hydrogel contact lenses for keratoconus incorporating correction for vertical coma aberration. 321–329 (2009) doi:10.1111/j.1475-1313.2009.00645.x.
51. Lee, B. Y. & Braun, P. V. Tunable Inverse Opal Hydrogel pH Sensors \*\*. 563–566 (2003) doi:10.1002/adma.200304588.
52. Ha, E. *et al.* Purification of His-tagged proteins using Ni <sup>2+</sup> – poly ( 2-acetamidoacrylic acid ) hydrogel. **876**, 8–12 (2008).
53. Sannino, A., Demitri, C. & Madaghiele, M. Biodegradable cellulose-based hydrogels: Design and applications. *Materials (Basel)*. **2**, 353–373 (2009).
54. “Smart” Materials Based on Cellulose A Review of the Preparations, Properties, and Applications.pdf.
55. Ross, R. J. & USDA Forest Service., F. P. L. *Wood handbook : wood as an engineering material*. *Circulation Research* vol. 39 https://www.ahajournals.org/doi/10.1161/01.RES.39.4.523 (2010).
56. The Rainforest Alliance. What is Sustainable Forestry. *What is Sustainable Forestry* https://www.rainforest-alliance.org/articles/what-is-sustainable-forestry (2016).
57. Cellulose Ethers and Esters | Article about Cellulose Ethers and Esters by The Free Dictionary. https://encyclopedia2.thefreedictionary.com/Cellulose+Ethers+and+Esters.
58. Dow. Methocel Cellulose Ethers. Technical Handbook.
59. Bonetti, L., De Nardo, L. & Farè, S. Thermo-Responsive Methylcellulose Hydrogels: From Design to Applications as Smart Biomaterials. *Tissue Eng. Part B Rev.* 1–94 (2020) doi:10.1089/ten.teb.2020.0202.

60. Zheng, P., Li, L., Hu, X. & Zhao, X. Sol-gel transition of methylcellulose in phosphate buffer saline solutions. *J. Polym. Sci. Part B Polym. Phys.* **42**, 1849–1860 (2004).
61. Methyl cellulose | 9004-67-5. [https://www.chemicalbook.com/ChemicalProductProperty\\_EN\\_CB3474718.htm](https://www.chemicalbook.com/ChemicalProductProperty_EN_CB3474718.htm).
62. Nasatto, P. L. *et al.* Methylcellulose, a cellulose derivative with original physical properties and extended applications. *Polymers (Basel)*. **7**, 777–803 (2015).
63. Joshi, S. C. & Lam, Y. C. Modeling heat and degree of gelation for methyl cellulose hydrogels with NaCl additives. *J. Appl. Polym. Sci.* **101**, 1620–1629 (2006).
64. Takahashi, M., Shimazaki, M. & Yamamoto, J. U. N. Thermoreversible Gelation and Phase Separation in Aqueous Methyl Cellulose Solutions. 91–100 (2000).
65. Funami, T., Kataoka, Y., Hiroe, M. & Asai, I. ARTICLE IN PRESS Thermal aggregation of methylcellulose with different molecular weights. **21**, 46–58 (2007).
66. Axelos, M. A. V, Rinaudo, M., Hirrien, M., Chevillard, C. & Desbrie, J. Thermogelation of methylcelluloses : new evidence for understanding the gelation mechanism. **39**, 6251–6259 (1998).
67. Methyl, I. V, Kato, T., Yokoyama, M. & Takahashi, A. Melting temperatures of thermally reversible gels. **21**, 15–21 (1978).
68. Sarkar, N. Kinetics of thermal gelation of methylcellulose and hydroxypropylmethylcellulose in aqueous solutions. **8617**, (1995).
69. Xu, Y., Wang, C., Tam, K. C. & Li, L. Salt-assisted and salt-suppressed sol-gel transitions of methylcellulose in water. *Langmuir* **20**, 646–652 (2004).
70. Nishinari, K. & Hofmann, K. E. Gel-sol transition of methylcellulose. **1226**, 1217–1226 (1997).
71. Sarkar, N., Polymers, D. & Dow, T. Thermal Gelation Properties of Methyl and Hydroxypropyl Methylcellulose \*. **24**, 1073–1087 (1979).
72. Hirrien, M., Desbriks, J. & Rinaudo, M. Physical properties of methylcelluloses in relation with the conditions for cellulose modification. **31**, 243–252 (1996).
73. Methylcellulose, a Cellulose Derivative with Original Physical Properties and Extended Applications \_ Enhanced Reader.pdf.
74. Xu, Y., Li, L., Zheng, P., Lam, Y. C. & Hu, X. Controllable gelation of methylcellulose by a salt mixture. *Langmuir* **20**, 6134–6138 (2004).
75. Kundu, P. P. & Kundu, M. Effect of salts and surfactant and their doses on the gelation of extremely dilute solutions of methyl cellulose. *Polymer (Guildf)*. **42**, 2015–2020 (2001).

76. Chen, C. H. *et al.* Novel living cell sheet harvest system composed of thermoreversible methylcellulose hydrogels. *Biomacromolecules* **7**, 736–743 (2006).
77. Contessi, N., Altomare, L., Filipponi, A. & Farè, S. Thermo-responsive properties of methylcellulose hydrogels for cell sheet engineering. *Mater. Lett.* **207**, 157–160 (2017).
78. Collins, K. D. Charge density-dependent strength of hydration and biological structure. *Biophys. J.* **72**, 65–76 (1997).
79. Israelachvili, J. N. Intermolecular and Surface Forces. شماره 8; ص 99-117  
[http://www.iust.ac.ir/files/fnst/ssadeghzadeh\\_52bb7/files/Israelachvili\\_J.N.-Intermolecular\\_and\\_surface\\_forces-AP\\_%282003%29.pdf](http://www.iust.ac.ir/files/fnst/ssadeghzadeh_52bb7/files/Israelachvili_J.N.-Intermolecular_and_surface_forces-AP_%282003%29.pdf) (1390).
80. Mamardashvili, G. M., Mamardashvili, N. Z. & Koifman, O. I. Synthesis and receptor properties of calix[4]pyrroles. *Russ. Chem. Rev.* **84**, 275–287 (2015).
81. Aston, R., Sewell, K., Klein, T., Lawrie, G. & Grøndahl, L. Evaluation of the impact of freezing preparation techniques on the characterisation of alginate hydrogels by cryo-SEM. *Eur. Polym. J.* **82**, 1–15 (2016).
82. Efthymiou, C., Williams, M. A. K. & Mcgrath, K. M. Food Hydrocolloids Revealing the structure of high-water content biopolymer networks : Diminishing freezing artefacts in cryo-SEM images. *Food Hydrocoll.* **73**, 203–212 (2017).